

April, 2022

The heavy tetra-quark states after the discovery of tetra-charm states.msifn

C. Becchi *

*Dipartimento di Fisica, Università di Genova
and
Istituto Nazionale di Fisica Nucleare, Sezione di Genova
via Dodecaneso 33, I-16146, Genoa, Italy*

Abstract

This paper is devoted to the study of exclusive charm and bottom aggregates which are suitable, at least partially, for a non-relativistic description. Starting from a simple choice of quarkonia and tetra-quark wave functions we study their production cross sections, total widths and more interesting decay properties.

In particular, we compute the production cross sections of the ground state scalar quarkonia getting results compatible with the values appearing in the literature. We also compute the production cross sections of the lower energy states of the charm and bottom tetra-quarks, their decay widths and the decay rates in two $\mu\bar{\mu}$ pairs and in the $q\bar{q}\mu\bar{\mu}$ channel.

Our results on the tetra-charm are consistent with the data published by the LHCb Collaboration and those on the tetra-bottom show a reasonable agreement with the indications published by the CMS Collaboration. Our cross section analyses are based on interpolations based on the gluon-gluon luminosity grids published by the NNPDF and CTEQ Collaborations. The hard amplitude calculations are based on QCD in the tree approximation. We think that a careful improvement of our method and a refinement of the experimental data after the foreseen luminosity increase at the LHC will make possible valuable tests of QCD at the intermediate energies.

*E-Mail: becchi@ge.infn.it

1 Introduction

The discovery of heavy quarkonia states $c\bar{c}$, $b\bar{b}$ and $c\bar{b}$ and the more recent detection of fully charmed tetra-quarks has revived the interest in non-relativistic quark physics since it turns out that the radius of the heavy quarkonia is larger than the quark Compton wavelength.

A natural consequence of this is the interest in fully heavy tetra-quark states. We shall denote by the capital letter Q the heavy Quarks. The physics of these compounds is expected to give important QCD tests if the internal kinetic energy is smaller than the Quark mass and hence the system can be considered non-relativistic. Thus Quarks can be considered fixed sources and the binding forces could be easily identified in lattice QCD also considering the many body forces [1].

In practice these considerations should concern the Quarks with masses of some GeV . Strictly speaking this weakly applies to the charm flavor while it is well satisfied by the bottom one. Top Quarks do not live long enough to feel inter quark binding forces.

We shall consider charmonium and bottomium states together with tetra-charm and tetra-bottom with the purpose of treating the whole multi-Quark physics in a coherent and consistent framework based on Quantum Field Theory in the non-relativistic limit. Quarkonia will give us interesting tests of our non-relativistic approach to the dynamics of both flavors that we shall also apply to tetra-Quarks. Clearly the first problem one must face with is the existence of bound or resonant tetra-Quark states. There are theoretical papers, partly based on lattice QCD, discussing this problem [2][3]. The role of many body forces is however rarely discussed [1].

Recently the discussion about the existence of tetra-Quarks has been intensified by the results published by the LHCb Collaboration [4] which, studying the production of double $\mu\bar{\mu}$ pairs, has found some evidence of tetra-charm resonances. In particular they have detected strong indications of resonances decaying into $Y(1S)\mu\bar{\mu}$ appearing over a background generated by the $\mu\bar{\mu}$ decay of pairs of J/ψ . We shall discuss this point in greater detail in the following.

Obviously, the existence of tetra-charm resonances should imply that of tetra-bottom ones because the short-distance Coulomb like forces act more strongly on the bottom Quarks.

Following the line of our former papers [5] and [6] we continue the analysis of the possibility of detecting the production of the tetra-bottom at the LHC. On account of [2] we shall assume in the non-relativistic approximation multi-Gaussian wave functions for both Quarkonia and tetra-Quarks of charm and bottom flavors. We shall denote by \mathcal{Q} the lower energy vector Quarkonia and by η_Q the pseudoscalar ones. Furthermore we shall denote by \mathcal{T}_Q the tetra-Quark states. For Quarkonia we shall choose the orbital wave function

$$\Psi_{\mathcal{Q}}(\vec{r}_1 - \vec{r}_2, \vec{P}) = \frac{1}{2^{\frac{3}{2}} \pi^{\frac{9}{4}} D_Q^{\frac{3}{2}}} e^{-\frac{(\vec{r}_1 - \vec{r}_2)^2}{2D_Q^2} + i\vec{P} \cdot \frac{\vec{r}_1 + \vec{r}_2}{2}}. \quad (1)$$

For the \mathcal{T}_Q states, following [2], we choose the product of three Gaussian factors, the first two factors depending respectively on the distance between the Quarks and that between the anti-Quarks. The third factor depends on the distance between the two Q and the two anti- Q

centers of mass. Taking into account the charge conjugation invariance we set

$$\Psi_{\mathcal{T}}(\vec{r}_1, \vec{r}_2, \vec{r}_3, \vec{r}_4, \vec{P}) = \frac{1}{2^{\frac{3}{2}} \pi^{\frac{15}{4}} d^3 \delta^{\frac{3}{2}}} e^{-\frac{(\vec{r}_1 + \vec{r}_2 - \vec{r}_3 - \vec{r}_4)^2}{8d^2} - \frac{(\vec{r}_1 - \vec{r}_2)^2 + (\vec{r}_3 - \vec{r}_4)^2}{2d^2}} e^{i\vec{P} \cdot \frac{\vec{r}_1 + \vec{r}_2 + \vec{r}_3 + \vec{r}_4}{4}} . \quad (2)$$

Clearly this choice of the wave functions is based on the non-relativistic character of the heavy Quark states.

We shall compute in Chapter 2 the radii D_Q of Quarkonia from their decay rate into $\mu\bar{\mu}$ pairs. But once assumed the form of the wave functions it is natural to compute their parameters by the variational method. However this requires a good knowledge of the masses and of the potential energies. As a matter of fact the values of the constituent masses of the heavy Quarks can be found in the literature where one finds the charm mass value $m_c = 1.55 \text{ GeV}$ and the value of the bottom mass $m_b = 4.73 \text{ GeV}$.

Concerning the potential energies, as discussed in [1] the dual superconductor model of the QCD vacuum implies that the tetra-Quark binding forces at large distances are generated by a constant tension string similar in shape to the capital H letter connecting a pair of Quarks in color triplet state on one side to a pair of anti-Quarks also in color triplet state on the other side. According to the lattice calculations [1] the value of the string tension should be about $\sigma = .16 \text{ GeV}^2$.

Assuming orbital S waves as in Eq. (2) both Quarks and anti-Quarks must be in spin triplet states, thus there should exist nine lower energy states with total angular momentum ranging from zero to two and mass differences of the order of magnitude of 100 MeV . This corresponds to less than 1% of the average mass which should lie near 6 GeV for the tetra-charm and 20 GeV for the tetra-bottom. The same ratio of the mass differences to the average mass appears between vector and pseudoscalar heavy Quarkonia.

At short distances the binding energy is dominated by Coulomb like two body forces whose strength, the QCD strong coupling $\alpha_S(Q^2)$, depends on the momentum transfer and hence on the radius of the bound state [7]. As a matter of fact the theoretical effective value of $\alpha_S(1/D^2)$ at the considered momentum transfer values is quite uncertain. However the variational method gives a relation between the values of the constituent quark mass m_Q , the quarkonium radius D_Q , the string tension σ and $\alpha_S(1/D_Q^2)$. The relations is

$$\frac{8 \alpha_S}{3\sqrt{\pi}} = \frac{3}{m_Q D_Q} - \frac{2\sigma}{\sqrt{\pi}} D_Q^2 . \quad (3)$$

Knowing the Quarkonium radii, i.e. $D_c = 1.6 \text{ GeV}^{-1}$ for the charmonium and $D_b = .8 \text{ GeV}^{-1}$ for the bottomium, Equation (3) gives the value of α_S appropriate for the two Quarkonia. We shall assume the same values for the corresponding tetra-Quarks because the average distances and hence the exchanged momenta are essentially the same for Quarkonia and tetra-Quarks.

The same variational method allows the determination of the tetra-Quark wave function

parameters d and δ identifying the minima in the positive quadrant of the function ¹

$$E(d, \delta) \equiv \frac{3}{4 m_Q} \left(\frac{1}{\delta^2} + \frac{4}{d^2} \right) + \frac{2\sigma}{\sqrt{\pi}} (d + 1.6 \delta) - \frac{8 \alpha_S}{3\sqrt{\pi}} \left(\frac{1}{d} + \sqrt{\frac{2}{2 d^2 + \delta^2}} \right). \quad (4)$$

It is apparent that the two equations identify uniquely the parameters d and δ as functions of the tension σ . In particular for the assumed value of the tension and α_S we find for the tetra-charm $\delta_c = 1.44 \text{ GeV}^{-1}$ and $d_c = 1.87 \text{ GeV}^{-1}$, while for the tetra-bottom we find $\delta_b = .803 \text{ GeV}^{-1}$ and $d_b = 1.01 \text{ GeV}^{-1}$.

In Chapter 3 we shall recall the properties of the lower energy states of tetra-Quarks that we have already discussed in references [5] and [6]. We shall represent these states in the second quantized form.

Once chosen the wave functions we can compute the more interesting decay processes of the Quarkonia and tetra-Quarks using the effective Hamiltonians which are computed in the appendices applying quantum field theory in the semi-classical (tree) approximation and in the non-relativistic framework for the heavy Quarks which is discussed in Appendix A.

A further important subject in the physics of the heavy-Quark compound states is their production cross section in the proton-proton collisions. In the parton model colliding protons appear as showers of partons, i.e. quarks, anti-quarks and gluons, whose momenta are essentially collinear^{2, 3}. The production of a heavy particle can be seen as the fusion of two partons, one from each proton, creating the heavy particle. This is the Drell-Yan mechanism which is clearly described in reference [11].

In Chapter 4 we recall how the Drell-Yan production cross section of a particle of mass M is related to the product of the modulus square of the transition amplitude between the two partons and the heavy particle and the luminosity [7] of the crossing parton showers. The parton-parton luminosity is given by the convolution integral of two parton distribution functions which depend on the Bjorken variables x_i , $i = 1, 2$ of the two partons and on the scale which is usually identified with the invariant mass of the two parton system, that

¹Notice that in the above function the term corresponding to the string energy has been approximated replacing the average minimal length of the string by $d + 1.6 \delta$. With regard to this choice notice that if the vectors joining the two (anti-)quarks that we denote by $\vec{\rho}$ and $\vec{\rho}'$ and that joining the center of mass of the two pairs that we denote by \vec{R} are parallel the minimal string length is $R + (\rho + \rho')/2$, while if they are orthogonal the length is $R + (4 - \sqrt{3})(\rho + \rho')/2$.

²In order to evaluate the corrections due to non-vanishing transverse parton momenta \vec{p}_t we must know the mean square value $\overline{p_t^2}$ of \vec{p}_t . Assuming a normal transverse momentum distribution we can get an estimate of $\overline{p_t^2}$ of the produced η_c at the LHCb from references [8] which give the η_c production cross section without any transverse momentum selection and that for transverse momentum $p_t > 6.5 \text{ GeV}$, the first cross section being $\sigma(0) \simeq 25.4 \pm 7.7 \mu b$ while the second one amounts to $\sigma(6.5) \simeq 1.26 \pm .33 \mu b$. From these data we can evaluate the mean square value of the η_c transverse momenta getting $\overline{p_t^2} \sim 14 \text{ GeV}^2 \sim 1.5 m_{\eta_c}^2$. Other experiments concerning the p_t distributions give $\overline{p_t^2} \sim 40 \text{ GeV}^2 \sim .4 m_{\Upsilon}^2$ for the Υ [9] and $\overline{p_t^2} \sim 10^3 \text{ GeV}^2 \sim .4 m_Z^2$ for the intermediate boson Z [10]. The most obvious correction due to p_t is the Lorentz contraction of the cross section. This corresponds to a correction of roughly $-\overline{p_t^2}/(m^2(1 + \exp(2y)))$, that is to less than -12% for the η_c at the LHCb and less than -9% for the η_b at the CMS apparatuses. These are of the order of the relativistic corrections.

³We systematically sum statistical and systematic errors.

is, in the collinear case, with $M^2 \equiv sx_1x_2$ where \sqrt{s} is the proton-proton collision energy. The convolution integral is in fact the integral over the gluon pair rapidity $y = \ln(x_1/x_2)/2$, and hence over the final particle rapidity, of the product of the parton distribution functions multiplied by the acceptance function of the experimental apparatus. The product of the parton distribution functions (PDF's) is usually called the differential parton-parton luminosity and is a function of y and M . In our case the partons which dominate the production mechanism are gluons. Thus we need the gluon-gluon luminosities for the LHC at $\sqrt{s} = 13 \text{ TeV}$ which can be computed from the literature, in particular, from the references [11], [12] and [13] ⁴.

On the basis of the results of Chapter 4 and of Appendices B and D in Section 4.1 we present the calculation in a generic heavy flavor case of the ratio \mathcal{R} of the resonant production of two $\mu\bar{\mu}$ pairs to the production due to the $\mu\bar{\mu}$ decay of two Quarkonia \mathcal{Q} .

In Section 4.2 we shall compare and discuss the gluon-gluon luminosities giving the values we shall use in our cross section calculations. In particular, taking into account the published results, we discuss the values of the gluon-gluon luminosities at the scales 3 GeV and 6 GeV for the LHCb apparatus and 10 GeV and 20 GeV for the CMS apparatus.

In Chapter 5, using our evaluations of the transition amplitudes $\eta \leftrightarrow 2g$, $\mathcal{T} \leftrightarrow 2g$ in Appendix D.1 and $\mathcal{T} \leftrightarrow q\bar{q}$ in Appendix D.2, we compute the production cross sections of η_Q 's and tetra-Quarks. We also compute the rates of the most important decay processes among which those into two $\mu\bar{\mu}$ pairs of the tetra-Quarks are the easiest to compute and the most interesting from the experimental point of view.

Unfortunately we have not been able to find among the LHC publications data about the prompt η_b production cross section ⁵. Indeed the knowledge of the prompt η_b production cross section would have given us a further, more reliable, test of our calculations at the 10 GeV scale.

Together with the production cross section of tetra-Quarks we compute in both flavor cases the value of the ratio \mathcal{R} of the resonant production cross section of double $\mu\bar{\mu}$ pairs to that of production of pairs of Quarkonia decaying into $\mu\bar{\mu}$ pairs. The measured value of double J/ψ production cross section in the rapidity interval $2 < y < 4.5$ has been published by the LHCb Collaboration in [16]. The same Collaboration has studied in the same rapidity interval [4] the invariant mass distribution of double $\mu\bar{\mu}$ pairs candidates for J/ψ decay in the interval $6.2 < M_{di-J/\psi} < 7.4 \text{ GeV}$ showing the presence of possibly two tetra-charm resonances. In the same paper the widths of the detected tetra-charm resonances is given, however with a wide uncertainty due to the possibility of interference of the resonance with the continuum background.

Considering the ratio \mathcal{R} in the bottom case we have referred to the CMS Collaboration which has measured the double Υ production cross section at the LHC energy $s = 13 \text{ TeV}$ [17]. This Collaboration gives for the double Υ production cross section, in the rapidity interval $-2 < y < 2$, the value of roughly 79 pb . The same paper, which studies the decays into double

⁴PDFs are released by individual groups as discrete grids of functions of the Bjorken- x and energy scale M . The LHAPDF project [14] maintains a repository of PDFs from various groups in a new standardized LHAPDF6 format, additional formats such as the CTEQ PDS grid format [12] are also in use.

⁵In particular there is no reference to the η_b in [15] where the production cross section of bottom pairs is presented.

$\mu\bar{\mu}$ pairs, also considers the possible appearance of \mathcal{T} resonances giving an upper bound for the product of production cross section times the decay branching fraction in two $\mu\bar{\mu}$ pairs which should not exceed 5 pb . We shall show that the detection of tetra-bottom resonances looks very difficult due to the small values of the production cross sections of bottom compound states.

On the contrary the resonant production of $Q\bar{Q}\mu\bar{\mu}$ that we study in Appendix B.2 could be identified using "b-tagging" of $b\bar{b}$ pairs near they threshold. However, the efficiency of "b-tagging" at about 1 GeV above threshold seems to be very small for transverse momenta of few GeV .

Beyond the electromagnetic decays we study the strong decays into gluons and light quarks. We shall also consider in Appendix C interesting channels such as the tetra-Quark decays into a $Q\bar{Q}$ pair together with two gluons or a light quark pair. From the lower order calculations the branching ratios in these channels turn out to be the larger ones. Therefore they give the most important contributions to the width of tetra-Quarks.

Particularly interesting is the calculation of the decay rates of the Quarkonia η_Q into two gluons which should give the larger contribution to the width of these scalar Quarkonia thus allowing a direct comparison with experimental results and hence a test of our method. The results based on the values of $\alpha_S(m_Q^2)$ given by [18] give $\Gamma_{\eta_c} \simeq 25\text{ MeV}$, and $\Gamma_{\eta_b} \simeq 4.6\text{ MeV}$ which are consistent with the Particle Data Book data.

All these calculations shall be limited to the hard part of the amplitudes, that concerning high momentum transfers and elementary constituents. What we miss is hadronization, however this is unavoidable. Consider for example the η_c decays, there are more than fifteen final channels containing two, three and four, particles. Therefore the quarks and gluons in the final states must be related to clusters of particles. Of course, hadronization modifies the rates but it should not change the order of magnitude of the results as it happens for the Quarkonia decay rates.

We shall systematically assign to the Quarkonia the mass $2m_Q$ and to the tetra-Quarks the mass $4m_Q$. We think that the errors due to these simplifying choices are negligible in the framework of the considered approximations.

2 $Q \rightarrow \mu\bar{\mu}$ decays and Quarkonic radii.

In order to determine the radii of Quarkonia D appearing in the wave function given in Eq. (1) we begin our analysis computing the rate of the decay $Q \rightarrow \mu\bar{\mu}$.

Due to the Q annihilation nature of the processes we shall represent the states in the Fock space and we shall use the transition Hamiltonian given in Eq. (45), in Appendix A. In the rest frame of the initial state the effective Hamiltonian takes into account that the momenta of the Quarks are negligible with respect of their masses. We use the golden rule as in [7]. The initial state with momentum \vec{P} and $j_z = 1$ is given by

$$\begin{aligned} |Q, 1, \vec{P}\rangle &= \frac{1}{\sqrt{3}} \int d\vec{r}_1 d\vec{r}_2 \Psi_Q(\vec{r}_1 - \vec{r}_2, \vec{P}) \tilde{A}_{+,a}^\dagger(\vec{r}_1) \tilde{B}_{+,a}^\dagger(\vec{r}_2) |0\rangle \\ &= \frac{1}{\sqrt{3} 2^{\frac{3}{2}} \pi^{\frac{9}{4}} D^{\frac{3}{2}}} \int d\vec{r}_1 d\vec{r}_2 e^{i\vec{P} \cdot \frac{\vec{r}_1 + \vec{r}_2}{2}} e^{-\frac{(\vec{r}_1 - \vec{r}_2)^2}{2D^2}} \tilde{A}_{+,a}^\dagger(\vec{r}_1) \tilde{B}_{+,a}^\dagger(\vec{r}_2) |0\rangle, \end{aligned} \quad (5)$$

while the scalar Quarkonium state is

$$|\eta_Q, \vec{P}\rangle = \frac{1}{\sqrt{3} 4\pi^{\frac{9}{4}} D^{\frac{3}{2}}} \int d\vec{r}_1 d\vec{r}_2 e^{i\vec{P} \cdot \frac{\vec{r}_1 + \vec{r}_2}{2}} e^{-\frac{(\vec{r}_1 - \vec{r}_2)^2}{2D^2}} [A_{+,a}^\dagger(\vec{r}_1) \tilde{B}_{-,a}^\dagger(\vec{r}_2) - A_{-,a}^\dagger(\vec{r}_1) \tilde{B}_{+,a}^\dagger(\vec{r}_2)] |0\rangle. \quad (6)$$

Therefore in the rest frame of \mathcal{Q} the transition amplitude is given by

$$\langle 0 | b_{\lambda'}(\vec{q}_2) a_{\lambda}(\vec{q}_1) H_I | \mathcal{Q}, 1, \vec{0} \rangle = - \frac{\alpha \zeta}{\sqrt{3} 2^{\frac{5}{2}} \pi^{\frac{5}{4}} m_Q^2 D^{\frac{3}{2}} \sqrt{q_1 q_2}} \delta(\vec{q}_1 + \vec{q}_2) (\bar{u}_{\lambda}(\vec{q}_1) (\gamma_x + i\gamma_y) v_{\lambda'}(\vec{q}_2)),$$

where ζ is the triple of the Quark electric charge, and the decay rate is given by

$$\begin{aligned} \Gamma_{\mathcal{Q} \rightarrow \mu\bar{\mu}} &\sim \frac{\alpha^2 \zeta^2}{3 2^4 \pi^{\frac{3}{2}} m_Q^4 D_{\Upsilon}^3} \int \frac{d\vec{k}}{k^2} \delta(2(k - m_b)) \text{Tr}(\not{k}(\gamma_x + i\gamma_y) \tilde{\not{k}}(\gamma_x - i\gamma_y)) \\ &= \frac{4 \alpha^2 \zeta^2}{9 \sqrt{\pi} D^3 m_Q^2} \simeq 0.25 \frac{\alpha^2 \zeta^2}{m_b^2 D^3}. \end{aligned} \quad (7)$$

Taking into account that in the Particle Data Books one finds $\Gamma_{J/\psi \rightarrow \mu\bar{\mu}} \sim 5.4 \text{ keV}$ and $\Gamma_{\Upsilon \rightarrow \mu\bar{\mu}} \sim 1.3 \text{ keV}$ we can compute the radius of Υ finding

$$D_{\Upsilon} \equiv D_b = \left(\frac{4 \alpha^2}{9 \sqrt{\pi} m_b^2 \Gamma_{\Upsilon \rightarrow \mu\bar{\mu}}} \right)^{\frac{1}{3}} \sim .8 \text{ GeV}^{-1}, \quad (8)$$

while for J/ψ we have

$$D_c = \left(\frac{16 \alpha^2}{9 \sqrt{\pi} m_c^2 \Gamma_{J/\psi \rightarrow \mu\bar{\mu}}} \right)^{\frac{1}{3}} \sim 1.6 \text{ GeV}^{-1}. \quad (9)$$

Now we can verify the validity of the non-relativistic approximation for both heavy flavors. Computing the product $m_Q^2 D_Q^2$ we find roughly 13 for the bottom and 6 for the charm. Therefore, we see that the non-relativistic approximation is more suitable for the bottom than for the charm but it should not be rejected even in the second case.

Now we consider the tetra-Quarks.

3 The states of the heavy tetra Quarks \mathcal{T}

Following the analysis in [5] and [6] we consider the ground states of a non-relativistic $QQ\bar{Q}\bar{Q}$ system that we denote by \mathcal{T} assuming that any internal angular momentum vanishes as it happens with the wave function given in Eq. (2).

QCD foresees that the most interacting states are those in which two anti-Quarks in color triplet, and hence with spin one, interact with two Quarks, in color anti-triplet and spin one. Thus we have nine possible states with total angular momentum 2, 1 and 0 and positive parity. The states with even angular momentum have positive charge conjugation while the others

have negative charge conjugation. There is also a state of null angular momentum in which Quarks combine in color sextets and anti-Quarks in color anti-sextets. However, according to the QCD string model this state should be less interacting.

The states with positive parity and charge conjugation should partially decay, even if with small branching ratio, in two $\mu\bar{\mu}$ pairs, as shown by the LHCb Collaboration. This is the channel of maximum signal to background ratio and hence most suitable for detection provided that the cross section be sufficient. A detailed discussion of these states and of their decay channel is contained in [5] and [6].

According to vector meson dominance the decay into two $\mu\bar{\mu}$ pairs is dominated by the two step tetra-Quark decay into a \mathcal{Q} with emission of a $\mu\bar{\mu}$ pair followed by the \mathcal{Q} decay into a further $\mu\bar{\mu}$ pair. The rate of the first decay step can be computed introducing the following Fock representation of the \mathcal{T} based on the space wave function given in Eq. (2). The tetra-Quark state with momentum \vec{P} , spin $J = 2, J_z = 2$, is given, understanding the sum over repeated color indices, by

$$|\mathcal{T}_2, 2, \vec{P}\rangle = \frac{1}{2\sqrt{3}} \int \prod_{i=1}^4 d\vec{r}_i \Psi_{\mathcal{T}}(\vec{r}_1, \vec{r}_2, \vec{r}_3, \vec{r}_4, \vec{P}) \tilde{A}_{+,a}^\dagger(\vec{r}_1) \tilde{A}_{+,b}^\dagger(\vec{r}_2) \tilde{B}_{+,a}^\dagger(\vec{r}_3) \tilde{B}_{+,b}^\dagger(\vec{r}_4) |0\rangle, \quad (10)$$

while the state with $J = 1, J_z = 1$ and momentum \vec{P} is given by

$$|\mathcal{T}_1, 1, \vec{P}\rangle = \frac{1}{2\sqrt{3}} \int \prod_{i=1}^4 d\vec{r}_i \Psi_{\mathcal{T}}(\vec{r}_1, \vec{r}_2, \vec{r}_3, \vec{r}_4, \vec{P}) \left[\tilde{A}_{+,a}^\dagger(\vec{r}_1) \tilde{A}_{+,b}^\dagger(\vec{r}_2) \tilde{B}_{+,a}^\dagger(\vec{r}_3) \tilde{B}_{-,b}^\dagger(\vec{r}_4) - \tilde{A}_{+,a}^\dagger(\vec{r}_1) \tilde{A}_{-,b}^\dagger(\vec{r}_2) \tilde{B}_{+,a}^\dagger(\vec{r}_3) \tilde{B}_{+,b}^\dagger(\vec{r}_4) \right] |0\rangle, \quad (11)$$

and the state with $J = 0$ and momentum \vec{P} is

$$|\mathcal{T}_0, \vec{P}\rangle = \frac{1}{6} \int \prod_{i=1}^4 d\vec{r}_i \Psi_{\mathcal{T}}(\vec{r}_1, \vec{r}_2, \vec{r}_3, \vec{r}_4, \vec{P}) \left[\tilde{A}_{+,a}^\dagger(\vec{r}_1) \tilde{A}_{+,b}^\dagger(\vec{r}_2) \tilde{B}_{-,a}^\dagger(\vec{r}_3) \tilde{B}_{-,b}^\dagger(\vec{r}_4) + \tilde{A}_{-,a}^\dagger(\vec{r}_1) \tilde{A}_{-,b}^\dagger(\vec{r}_2) \tilde{B}_{+,a}^\dagger(\vec{r}_3) \tilde{B}_{+,b}^\dagger(\vec{r}_4) - \tilde{A}_{+,a}^\dagger(\vec{r}_1) \tilde{A}_{-,b}^\dagger(\vec{r}_2) \tilde{B}_{+,a}^\dagger(\vec{r}_3) \tilde{B}_{-,b}^\dagger(\vec{r}_4) - \tilde{A}_{-,a}^\dagger(\vec{r}_1) \tilde{A}_{+,b}^\dagger(\vec{r}_2) \tilde{B}_{-,a}^\dagger(\vec{r}_3) \tilde{B}_{+,b}^\dagger(\vec{r}_4) \right] |0\rangle. \quad (12)$$

4 The Drell-Yan production cross sections.

In the Appendices D.1 and D.2 we compute the transition amplitudes between tetra-Quarks and the parton pairs for which the LHC luminosity [11] is larger, these amplitudes are $\mathcal{T}_0 \rightarrow 2g$, $\mathcal{T}_2 \rightarrow 2g$, $\mathcal{T}_0 \rightarrow q\bar{q}$ and $\mathcal{T}_2 \rightarrow q\bar{q}$.

We identify the transition amplitudes in the \mathcal{T} rest frame with the matrix elements of the T operator which corresponds to the effective Hamiltonian through the relation [7]

$$\langle F | H_{eff} | I \rangle = \langle F | T | I \rangle \delta(\vec{P}_I - \vec{P}_F).$$

We further remind that, if the parton masses are negligible, the invariant transition amplitude is given by

$$\mathcal{M}_{\mathcal{T} \rightarrow 2p} = -4 (\pi M_{\mathcal{T}})^{\frac{3}{2}} T_{\mathcal{T} \rightarrow 2p}.$$

Once the two-partons-to- \mathcal{T} transition amplitudes are known we can compute the Drell-Yan production cross sections of \mathcal{T} at the LHC in terms of the parton-parton luminosities.

Forgetting for simplicity the dependence on transverse momenta we denote by ϵ_1 and ϵ_2 the parton energies and we compute the contribution of a \mathcal{T} exchange in the s channel to the forward invariant scattering amplitude of the two partons with fixed helicities

$$\mathcal{M}_{2-2} = \frac{|\mathcal{M}_{\mathcal{T} \rightarrow 2p}|^2}{(s - M_{\mathcal{T}}^2 - 2i\Gamma_{\mathcal{T}}M_{\mathcal{T}})} .$$

The S matrix unitarity implies that the production cross section of a \mathcal{T} with given angular momentum by two partons is given by

$$\hat{\sigma}_0 = -i \frac{\mathcal{M}_{2-2} - \mathcal{M}_{2-2}^*}{8\epsilon_1\epsilon_2} .$$

The \mathcal{T} width $\Gamma_{\mathcal{T}}$ being much smaller than m_Q we get for a single \mathcal{T} component at its threshold

$$\bar{\sigma}_0 = 2\pi \overline{|\mathcal{M}_{\mathcal{T} \rightarrow 2p}|^2} \frac{\delta(4\epsilon_1\epsilon_2 - M_{\mathcal{T}}^2)}{8\epsilon_1\epsilon_2} = 16\pi^4 M_{\mathcal{T}} \overline{|T_{\mathcal{T} \rightarrow 2p}|^2} \delta(4\epsilon_1\epsilon_2 - M_{\mathcal{T}}^2) ,$$

where we have introduced the average over the parton helicities and colors. Lorentz invariance implies that the \mathcal{T} production cross section does not depend on its rapidity.

Introducing the Bjorken variables by $\epsilon_i = x_i p$ and the square center of mass the LHC energy $s = 4p^2$, the square center of mass energy of the partonic process is given by $4\epsilon_1\epsilon_2 = x_1x_2s \equiv \tau s$ while the center of mass rapidity is given by $y = \ln(x_1/x_2)/2$. If $f_g(x_i, \mu)$ is the g -partonic density the integrated \mathcal{T} production cross section is

$$\begin{aligned} \sigma_{\mathcal{T}} &\simeq 16\pi^4 M_{\mathcal{T}} \overline{|T_{\mathcal{T} \rightarrow 2p}|^2} \int_0^1 dx_1 dx_2 \Theta(x_1, x_2) f_g(x_1, M_{\mathcal{T}}) f_g(x_2, M_{\mathcal{T}}) \delta(x_1x_2s - M_{\mathcal{T}}^2) \\ &= 16\pi^4 M_{\mathcal{T}} \overline{|T_{\mathcal{T} \rightarrow 2p}|^2} \frac{1}{s} \int_{-\ln \frac{\sqrt{s}}{M_{\mathcal{T}}}}^{\ln \frac{\sqrt{s}}{M_{\mathcal{T}}}} dy \Theta(y) f_g\left(\frac{M_{\mathcal{T}}}{\sqrt{s}} e^y, M_{\mathcal{T}}\right) f_g\left(\frac{M_{\mathcal{T}}}{\sqrt{s}} e^{-y}, M_{\mathcal{T}}\right) , \end{aligned} \quad (13)$$

where the Θ functions account for the acceptance of the experimental apparatuses.

As a matter of fact in reference [11] one finds the full luminosities corresponding for us to $|y| < 6.5 = \ln \frac{\sqrt{s}}{M_{\mathcal{T}_b}}$. On the contrary we must consider that at the CMS the luminosity is restricted to $|y| < 2$ while at the LHCb it is restricted to the interval $2 \leq y \leq 4.5$.

Disregarding the acceptance reductions due to cuts on the transverse momenta applied by the experimental apparatuses [17], for simplicity and for the incompleteness of our information, we can evaluate the gluonic luminosity which is given by

$$\frac{\partial L}{\partial M^2}(M) = \frac{1}{s} \int_{-\ln \frac{\sqrt{s}}{M}}^{\ln \frac{\sqrt{s}}{M}} dy \Theta(y) f_g\left(\frac{M}{\sqrt{s}} e^y, M\right) f_g\left(\frac{M}{\sqrt{s}} e^{-y}, M\right) . \quad (14)$$

If the partons are light quark pairs $q\bar{q}$ the luminosity lessens by two orders of magnitude that of gluon pairs.

Using the mean square transition amplitudes given in Eq.s (72) , (73) and (76) in the Appendices D.1 and D.2 and using Eq. (13) together the values of luminosities given in the third row of Table 1 we compute the production cross sections of the most interesting states of tetra-Quarks. Taking into account that \mathcal{T}_2 has the spin multiplicity equal to 5 we get the contribution of gluons to the cross section

$$\sigma_{\mathcal{T}_2} \simeq 80 \pi^4 M_{\mathcal{T}} \overline{|T_{\mathcal{T}_2 \rightarrow 2g}|^2} \frac{\partial L_{2p}}{\partial M_{\mathcal{T}}^2}(M_{\mathcal{T}}) \simeq 17 \sigma_{\mathcal{T}_0} , \quad (15)$$

where, from Equation (73), we have

$$\overline{|T_{\mathcal{T}_2 \rightarrow 2g}|^2} \simeq 3.4 \cdot 10^{-3} \frac{\alpha_S^4}{m_Q^{10} d^6 \delta^3} . \quad (16)$$

For the above-mentioned reasons concerning the light quark luminosity and taking into account Eq. (76) we can conclude that the light quark contributions to the cross section are negligible.

4.1 The signal to background ratio for tetra-Quark decay into two $\mu\bar{\mu}$ pairs.

The possibility of detecting a \mathcal{T} critically depends on the background in the chosen decay channel. According to [4] the best choice is the channel of two $\mu\bar{\mu}$ pairs, each pair having a center of mass energy not far from the mass of the corresponding Quarkonium \mathcal{Q} . In this decay channel the background is mainly due to the production of pairs of \mathcal{Q} both decaying into $\mu\bar{\mu}$ pairs. Therefore the signal to background ratio is strictly related to the ratio \mathcal{R} between the rate of two $\mu\bar{\mu}$ pair production from the tetra-Quark decays and that from the production of pairs of Quarkonia decaying into $\mu\bar{\mu}$ pairs. If in the calculation of \mathcal{R} we distinguish the contribution from tetra-Quarks of different spin, that is we write $\mathcal{R} = \mathcal{R}_2 + \mathcal{R}_0$, for each term we have

$$\mathcal{R}_J = \frac{\sigma_{\mathcal{T}_J} B_{\mathcal{T}_J \rightarrow 2\mu 2\bar{\mu}}}{\sigma_{2\mathcal{Q}} B_{\mathcal{Q} \rightarrow 2\mu}^2} , \quad (17)$$

where $B_{\mathcal{T}_J \rightarrow 2\mu 2\bar{\mu}}$ and $B_{\mathcal{Q} \rightarrow 2\mu}$ are the decay branching ratios into $\mu\bar{\mu}$ pairs of the tetra-Quark and of the Quarkonium.

The LHCb Collaboration has measured, albeit with big uncertainties, the ratio \mathcal{R} for the tetra-charm [4], the same Collaboration has measured [16] the production cross section of Quarkonium pairs $\sigma_{2J/\psi}$.

Our calculations of \mathcal{R} for \mathcal{T}_2 and \mathcal{T}_0 are based on Eq. (51) in Appendix B.1 , that is

$$\Gamma_{\mathcal{T}_2 \rightarrow \mathcal{Q}\mu\bar{\mu}} \simeq \frac{2^{\frac{19}{2}} d^3 \delta^3 D^6}{3(4d^2\delta^2 + D^2(d^2 + 2\delta^2))^3} \Gamma_{\mathcal{Q} \rightarrow \mu\bar{\mu}} \simeq 4 \Gamma_{\mathcal{T}_0 \rightarrow \mathcal{Q}\mu\bar{\mu}} ,$$

from which, assuming vector meson dominance, we have the following decay rate of \mathcal{T}_2 into two $\mu\bar{\mu}$ pairs

$$\Gamma_{\mathcal{T}_2 \rightarrow 2\mu 2\bar{\mu}} \simeq \frac{2^{\frac{19}{2}} d^3 \delta^3 D^6}{3(4d^2\delta^2 + D^2(d^2 + 2\delta^2))^3} \frac{\Gamma_{\mathcal{Q} \rightarrow \mu\bar{\mu}}^2}{\Gamma_{\mathcal{Q}}} .$$

Therefore the \mathcal{R}_J ratios are given by

$$\mathcal{R}_2 \simeq \frac{2^{\frac{19}{2}} d^3 \delta^3 D^6}{3(4d^2\delta^2 + D^2(d^2 + 2\delta^2))^3} \frac{\sigma_{\mathcal{T}_2}}{\Gamma_{\mathcal{T}_2}} \frac{\Gamma_{\mathcal{Q}}}{\sigma_{2\mathcal{Q}}} \simeq 5.7 \mathcal{R}_0 . \quad (18)$$

The Quarkonium widths $\Gamma_{\mathcal{Q}}$ can be found in Particle Data Books while the cross sections $s_{2\mathcal{Q}}$ are given in [16] for the charmonium pairs and in [17] for the production of the bottomium pairs at the LHC energy $\sqrt{s} = 13 \text{ TeV}$. In order to complete the calculation we need the tetra-Quark widths $\Gamma_{\mathcal{T}}$ which we approximate to their strong decay rates at the first orders in α_S . The \mathcal{T} decay rates $\mathcal{T}_J \rightarrow Q\bar{Q}2g$ and $\mathcal{T}_2 \rightarrow Q\bar{Q}q\bar{q}$ are computed in Appendix C, Eq.s (64), (65), (67) and (68). The third order corrections are expected to be 10% corrections. Therefore, we shall limit our calculation to the second order in α_S and use Eq. (66)

$$\Gamma_{\mathcal{T}_2} \simeq \frac{20 \alpha_S^2}{m_Q^2 (d^2 + 2\delta^2)^{\frac{3}{2}}} \simeq 3 \Gamma_{\mathcal{T}_0} .$$

Using all the above data and equations together with Eq.s (15) and (22) where we replace $M_{\mathcal{T}}$ with $4m_Q$, we find

$$\mathcal{R}_2 \simeq 1.7 \cdot 10^3 \frac{(d^2 + 2\delta^2)^{\frac{3}{2}}}{(4d^3\delta^2 + d D^2(d^2 + 2\delta^2))^3} \frac{\alpha_S^2(4m_Q^2) D^6}{m_Q^7} \frac{\Gamma_{\mathcal{Q}}}{\sigma_{2\mathcal{Q}}} \frac{\partial L_{2g}}{\partial M_{\mathcal{T}}^2} . \quad (19)$$

Remember that Quarkonium radii are computed in Chapter 2, Eq.s (8) and (9), where we find for the bottomium $D_b \simeq .8 \text{ GeV}^{-1}$ and for the charmonium $D_c \simeq 1.6 \text{ GeV}^{-1}$ while the tetra-Quark parameters are computed by the variational method getting for the charm flavor $\delta_c = 1.44 \text{ GeV}^{-1}$ and $d_c = 1.87 \text{ GeV}^{-1}$, while for the bottom we have $\delta_b = .803 \text{ GeV}^{-1}$ and $d_b = 1.01 \text{ GeV}^{-1}$. Taking into account the Quark masses we also have from [18] $\alpha_S(4m_c^2) \simeq .25$ and $\alpha_S(4m_b^2) \simeq .17$

The Quarkonium widths are given in the recent Particle Data Books where one finds $\Gamma_{J/\psi} \simeq 9.3 \cdot 10^{-5}$ and $\Gamma_{\Upsilon} \simeq 5.4 \cdot 10^{-5}$, while the production cross sections of \mathcal{Q} pairs at 13 TeV are given by the LHCb Collaboration in [16] $\sigma_{2J/\psi} \simeq 1.5 \cdot 10^4 \text{ pb}$ and by the CMS Collaboration in [17] $\sigma_{2\Upsilon} \simeq 79 \text{ pb}$.

4.2 The gluon-gluon luminosities.

The Drell-Yan production cross sections given in Equation (15) and thence the η_Q and \mathcal{T} production cross sections and the signal to background ratios \mathcal{R} given in Equation (19) are proportional to the gluon-gluon luminosities $\partial L / \partial M^2(M)$ as shown in Equation (14).

Thus we need the LHC gluon-gluon luminosity densities at $\sqrt{s} = 13 \text{ TeV}$ which are given in the literature, in particular, in the references [11], [12] and [13].

In Table 1 we report the luminosities seen by the apparatuses CMS and LHCb according to the data grills given by the Collaborations MSTW [11], NNPDF [13] and CTEQ [12] at the scales 3, 6, 10 and 20 GeV. Notice that at the scale 3 GeV the luminosities computed

from the data given by the MSTW collaboration are about ten times those computed by the Collaborations NNPDF and CTEQ, which essentially agree, while they decrease to the double of the same luminosities at the scale 20 GeV. Therefore, it is apparent that the extrapolations made by the MSTW Collaboration are based on different evolution equations from those used by the other two Collaborations. Notice also that the luminosities at the CMS are twice as much as those at the LHCb. In our calculations we shall use the more recent luminosities given by the Collaborations NNPDF and CTEQ. On account of the approximations made in the construction of our non-relativistic scheme the difference between the data obtained from the two references turns out to be scarcely relevant.

The knowledge of the gluon-gluon luminosities at $M \sim 3 \text{ GeV}$ and $M \sim 6 \text{ GeV}$ allows two tests of our non-relativistic approach which, however, are quite weak due to the smallness of M and the presence of transverse momenta of few GeV .

Our result on the η_c production cross section that we give in the next Chapter, i.e. $\sigma_{\eta_c} \simeq 39 \mu b$, must be compared with the experimental value of $25.4 \pm 7.7 \mu b$ which is obtained from the references listed in [8]. As a matter of fact the LHCb Collaboration has published in 2016 the prompt production cross section of a J/ψ and in 2020 that of an η_c with transverse momentum larger than 6.5 GeV . In the same publication it is given the ratio of the J/ψ to the η_c prompt production cross sections. The above given value of the η_c prompt production cross section is obtained comparing both publications. This comparison gives also an indication of the transverse momentum distribution of the produced Quarkonia and hence of the two-gluon transverse momentum distribution at the mass of 3 GeV . Assuming a Gaussian distribution we find a variance of $\overline{p_t^2} \sim 14 \pm 2.5 \text{ GeV}^2$. Apparently our result for σ_{η_c} is 1.56 times the experimental value of the production cross section even if we choose the smaller value, given in reference [11], of the luminosity.

A second test, which involves the LHCb gluon-gluon luminosity near 6 GeV given in Table 1, third line, consists in the comparison of the computed the tetra-charm ratio \mathcal{R}_c , whose value, given in the next Chapter, is about $2 \cdot 10^{-3}$ with the experimental value published by reference [4], which is $(1.1 \pm .57) \cdot 10^{-2}$ and hence compatible with any value of the ratio below $2.5 \cdot 10^{-2}$.

Therefore, in conclusion, we base our calculations on the gluon-gluon luminosities which are listed in Table 1 at the scales $M \sim 3 \text{ GeV}$ and $M \sim 6 \text{ GeV}$ at the LHCb and at the scales $M \sim 10 \text{ GeV}$ and $M \sim 20 \text{ GeV}$ at CMS. These are based on the data given by reference [11]. We remind that the gluon-gluon luminosities at the LHCb are worth half of those at CMS at

Apparatus-coll. \ Mass	3 GeV	6 GeV	10 GeV	20 GeV
LHCb-MSTW.n	$4 \cdot 10^{10}$	$6.14 \cdot 10^9$	$1.95 \cdot 10^9$	$2.9 \cdot 10^8$
LHCb-NNPDF.n	$5.74 \cdot 10^9$	$2.46 \cdot 10^9$	$9.28 \cdot 10^8$	$1.7 \cdot 10^8$
LHCb-CTEQ.n	$4.91 \cdot 10^9$	$2.43 \cdot 10^9$	$9.58 \cdot 10^8$	$1.88 \cdot 10^8$
CMS-MSTW.n	$6.32 \cdot 10^{10}$	$1.24 \cdot 10^{10}$	$4.29 \cdot 10^9$	$6.68 \cdot 10^8$
CMS-NNPDF.n	$7.5 \cdot 10^9$	$4.6 \cdot 10^9$	$2 \cdot 10^9$	$4 \cdot 10^8$
CMS-CTEQ.n	$8.1 \cdot 10^9$	$5.15 \cdot 10^9$	$2.23 \cdot 10^9$	$4.34 \cdot 10^8$

Table 1: Gluon-gluon luminosity table in picobarns as explained in the text below.

the same energy.

5 Numerical results on charm and bottom compound states

In this Chapter we give our results and comment their meaning for what concerns the possible detection of tetra-bottom states.

We use the parameters given in the Introduction, that is, for the charm flavor we have set $m_c = 1.55 \text{ GeV}$, $D_c = 1.6 \text{ GeV}^{-1}$, $\delta_c = 1.44 \text{ GeV}^{-1}$, $d_c = 1.87 \text{ GeV}^{-1}$ and for the bottom $m_b = 4.73 \text{ GeV}$, $D_b = .8 \text{ GeV}^{-1}$, $\delta_b = .803 \text{ GeV}^{-1}$, $d_b = 1.01 \text{ GeV}^{-1}$ together with the values of $\alpha_S(M^2)$ given in reference [18]. In particular we have set in units GeV^2 , $\alpha_S(2.4) = .32$, $\alpha_S(10) = .25$, $\alpha_S(22) = .21$, $\alpha_S(100) = .17$.

The first point we discuss concerns the reliability of the non-relativistic approximation for the scalar Quarkonia. Using Equation (49) in Appendix B we find the decay widths into two gammas

$$\Gamma_{\eta_c \rightarrow 2\gamma} = 7.2 \text{ keV}, \quad \text{and} \quad \Gamma_{\eta_b \rightarrow 2\gamma} = .38 \text{ keV} .$$

Taking into account the full widths given by the Particle Data Book we find the 2γ branching ratios

$$B_{\eta_c \rightarrow 2\gamma} = 4 \cdot 10^{-4} ,$$

to be compared with the ratio $4.3 \pm 1.5 \cdot 10^{-4}$ given by the Particle Data Book. As a matter of fact, the two values are perfectly compatible which is better than expected for the charm flavor.

In the bottom case, where the agreement between experiment and theory should be better, we find

$$B_{\eta_b \rightarrow 2\gamma} = 3.8 \pm 1.8 \cdot 10^{-5} ,$$

but no experimental value is given because the 2γ decay has not been seen.

Our calculations of the η_Q total width that we identify with the two-gluon decay width give the following results.

We begin from the η_c whose width computed in Appendix C, Equation (63), is

$$\Gamma_{\eta_c} = \frac{8\alpha_s^2(m_Q^2)}{3\sqrt{\pi}m_Q^2 D_Q^3} \simeq 25 \text{ MeV} , \quad (20)$$

that we have compared in the previous Section with the datum given by the Particle Data Book (i. e. $17.3 \pm 2.5 \text{ MeV}$) which is smaller but compatible with our result.

The same calculations for the η_b give the following decay width

$$\Gamma_{\eta_b} \simeq 4.6 \text{ MeV} , \quad (21)$$

which must be compared with the Particle Data Book value that is 10_{-4}^{+5} MeV . Let us note that both computed decay widths of the pseudoscalar Quarkonia reasonably agree with their experimental values.

Using furthermore the gluon-gluon luminosity values given in Table 1 we can compute the numerical values of the production cross sections of charm and bottom compound states.

The η_c production cross section σ_{η_c} is obtained introducing into Equation (15) the average square modulus of the transition amplitude to a gluon pair, which is obtained from Equation (15), that is

$$\overline{|T_{\eta_c \rightarrow 2g}|^2} \simeq \frac{\alpha_S^2(m_c^2)}{192 \ m_c^4 \pi^{\frac{5}{2}} D_c^3} , \quad (22)$$

and is directly related to the above given value of Γ_{η_c} . Using Equation (13), we have

$$\sigma_{\eta_c} \simeq \frac{\pi^{\frac{3}{2}} \alpha_S^2(m_c^2)}{6 \ m_c^3 \ D_c^3} \frac{\partial L}{\partial M^2} |_{LHCb(2m_c)} \simeq 8 \cdot 10^{-3} \frac{\partial L}{\partial M} |_{LHCb(3 \text{ GeV})} \simeq 39 \ \mu b , \quad (23)$$

while, as we have already said in the last Section, the cross section measured at the LHCb [8] is $\sigma_{\eta_c} \simeq 25.4 \pm 7.7 \ \mu b$. Also here our value is compatible with the experimental one within 2 σ , despite the low value of the final particle mass and hence the uncertainties in the gluon-gluon luminosity and those due to the relativistic corrections and to the transverse momenta corrections. Let us remind that, in particular for the charm data, our results are foreseen to give just the order of magnitude of the experimental values.

For the η_b prompt production cross section measured at CMS we get

$$\sigma_{\eta_b} \simeq \frac{\pi^{\frac{3}{2}} \alpha_S^2(m_b^2)}{6 \ m_b^3 \ D_b^3} \frac{\partial L}{\partial M} |_{CMS(2m_b)} \simeq 7.5 \cdot 10^{-4} \frac{\partial L}{\partial M^2} |_{CMS(10 \text{ GeV})} \simeq 1.7 \ \mu b . \quad (24)$$

We have not been able to find in the existing literature any published experimental value of this cross section which is quite smaller than that of η_c , let us hope that some new result will soon appear in spite of the very low detection efficiency of two gluon jets at 5 *GeV*.

Next we consider the tetra-Quark states beginning from the resonant production of two $\mu\bar{\mu}$ pairs from the \mathcal{T}_2 decay. We consider first the experimental datum from the LHCb Collaboration [4] which refers to the signal to background ratio \mathcal{R}_2 for the tetra-charm, where the background is due to the $\mu\bar{\mu}$ decay of a pair of vector Quarkonia. From Equation (19) with $\Gamma_{J/\psi} \simeq 9.3 \cdot 10^{-5}$ and using the production cross sections given by the LHCb Collaboration in [16], i.e. $\sigma_{2J/\psi} \simeq 1.5 \pm .2 \cdot 10^4 \ pb$, we have

$$\mathcal{R}_{c2} \simeq 8.7 \cdot 10^{-13} \frac{\partial L}{\partial M^2} |_{LHCb(6 \text{ GeV})} \simeq 5.7 \ \mathcal{R}_{c2} \simeq (2.1 \pm .2) \cdot 10^{-3} \quad (25)$$

while the values given in reference [4] vary between $(1.1 \pm .7) \cdot 10^{-2}$, without any p_T selection, and $(2.6 \pm 1.4) \cdot 10^{-2}$ for $p_T > 5.2 \text{ GeV}$.

Here our result, even being five times smaller, is compatible with the experimental indications. Furthermore we should consider the uncertainties of our result taking into account those due to the uncertain value of the gluon-gluon luminosity and those related to the presence of transverse momenta and to the need of relativistic corrections.

In the bottom case, taking into account that $\Gamma_{\Upsilon} \simeq 5.4 \cdot 10^{-5}$ and the production cross section given by the CMS Collaboration in [17], i.e. $\sigma_{2\Upsilon} \simeq 79 \pm 20 \ pb$, we get

$$\mathcal{R}_{b2} \simeq 3.4 \cdot 10^{-11} \frac{\partial L}{\partial M^2} |_{CMS(20 \text{ GeV})} \simeq (1.5 \pm .4) \cdot 10^{-2} , \quad (26)$$

which is worth seven times \mathcal{R}_{c2} . Still this result looks in agreement with what is shown in reference [17], Figure 7, which, however, has a significance of only one standard deviation. Perhaps an higher integrated luminosity might improve this agreement.

However in order to verify the possibility of repeating for the bottom flavor at CMS the LHCb Collaboration measure for the charm, one has to consider beyond the ratios \mathcal{R}_2 the value of the tetra-Quark production cross sections. From Equations (15) and (22) we get

$$\sigma_{\mathcal{T}_2} \simeq 139 \frac{\alpha_S^4}{m_Q^9 d_Q^6 \delta_Q^3} \frac{\partial L_{2g}}{\partial M^2}(4m_Q) \simeq 17 \sigma_{\mathcal{T}_0} , \quad (27)$$

thence, for the tetra-charm at the LHCb, we have

$$\sigma_{\mathcal{T}_{c2}} \simeq 17 \sigma_{\mathcal{T}_{c0}} \simeq 8.23 \cdot 10^{-5} \frac{\partial L_{2g}}{\partial M^2}|_{LHCb}(6 \text{ GeV}) \simeq .2 \mu b , \quad (28)$$

while for the tetra-bottom at CMS we have

$$\sigma_{\mathcal{T}_{b2}} \simeq 17 \sigma_{\mathcal{T}_{b0}} \simeq 1.9 \cdot 10^{-7} \frac{\partial L_{2g}}{\partial M^2}|_{CMS}(20 \text{ GeV}) \simeq 82 \text{ pb} , \quad (29)$$

which is about three orders of magnitude smaller than the tetra-charm cross section.

It is also important to compute the value of the \mathcal{T} width that from Equation (66) turns out to be

$$\Gamma_{\mathcal{T}_{c2}} \simeq 3 \Gamma_{\mathcal{T}_{c0}} \simeq 25 \text{ MeV} , \quad (30)$$

while for the tetra-bottom we have

$$\Gamma_{\mathcal{T}_{b2}} \simeq 3 \Gamma_{\mathcal{T}_{b0}} \simeq 7.3 \text{ MeV} . \quad (31)$$

Note that the width of a component (perhaps the $J = 2$ one) of the tetra-charm has been measured by the LHCb Collaboration [4] getting $\Gamma_{\mathcal{T}_{c?}} = 80 \pm 52 \text{ MeV}$ assuming no interference with the background and $\Gamma_{\mathcal{T}_{c?}} = 168 \pm 102 \text{ MeV}$ assuming interference. Our result is compatible with both experimental data.

Further results concerning the decay properties of the tetra-Quarks are obtained from Equation (52), getting for the tetra-charm

$$\begin{aligned} \Gamma_{\mathcal{T}_{c2} \rightarrow \Upsilon \mu \bar{\mu}} &\simeq 4 \Gamma_{\mathcal{T}_{c0} \rightarrow \Upsilon \mu \bar{\mu}} \simeq .69 \Gamma_{J/\psi \rightarrow \mu \bar{\mu}} \simeq 3.7 \text{ keV} , \\ \Gamma_{\mathcal{T}_{c2} \rightarrow 2\mu 2\bar{\mu}} &\simeq 4 \Gamma_{\mathcal{T}_{c0} \rightarrow 2\mu 2\bar{\mu}} \simeq .22 \text{ keV} , \end{aligned} \quad (32)$$

while for the tetra-bottom we get

$$\begin{aligned} \Gamma_{\mathcal{T}_{b2} \rightarrow \Upsilon \mu \bar{\mu}} &\simeq 4 \Gamma_{\mathcal{T}_{b0} \rightarrow \Upsilon \mu \bar{\mu}} \simeq .49 \Gamma_{\Upsilon \rightarrow \mu \bar{\mu}} \simeq .66 \text{ keV} , \\ \Gamma_{\mathcal{T}_{b2} \rightarrow 2\mu 2\bar{\mu}} &\simeq 4 \Gamma_{\mathcal{T}_{b0} \rightarrow 2\mu 2\bar{\mu}} \simeq 16 \text{ eV} , \end{aligned} \quad (33)$$

from which it clearly appears that the tetra-bottom detection in the decay into two $\mu \bar{\mu}$ pairs is much more difficult than the tetra-charm detection. Indeed, from Equations (29), (31) and (33), the resonant production cross section in two $\mu \bar{\mu}$ pairs due to the tetra-bottom turns out to

be $\sigma_{\mathcal{T}_{b2} \rightarrow 2\mu 2\bar{\mu}} \simeq .18 \text{ fb}$. The CMS Collaboration trying to measure this cross section has given in reference [17] an upper bound of 5 pb , more than four orders of magnitude above our result. However, assuming our cross section value and considering that [17] refers to an integrated luminosity of about 36 fb^{-1} which, taking into account the high $\mu\bar{\mu}$ pair detection efficiency of the apparatus, would correspond to about 7 events, what appears in Figure 7 in reference [17] seems reasonable.

We have already remarked that the tetra-Quark decay rate into a single $\mu\bar{\mu}$ pair together with a $Q\bar{Q}$ pair, which is computed in Equations (55) and (56), appears to be for the \mathcal{T}_c

$$\Gamma_{\mathcal{T}_{c2} \rightarrow Q, \bar{Q}, \mu\bar{\mu}} \simeq 4 \Gamma_{\mathcal{T}_{c0} \rightarrow Q, \bar{Q}, \mu\bar{\mu}} \simeq 4 \text{ keV} , \quad (34)$$

and for the \mathcal{T}_b

$$\Gamma_{\mathcal{T}_{b2} \rightarrow Q, \bar{Q}, \mu\bar{\mu}} \simeq 4 \Gamma_{\mathcal{T}_{b0} \rightarrow Q, \bar{Q}, \mu\bar{\mu}} \simeq .64 \text{ keV} . \quad (35)$$

Thus, the resonant production cross sections in the considered channel turn out to be for \mathcal{T}_c

$$\sigma_{\mathcal{T}_{c2} \rightarrow c, \bar{c}, \mu\bar{\mu}} \simeq 7.6 \sigma_{\mathcal{T}_{c0} \rightarrow c, \bar{c}, \mu\bar{\mu}} \simeq 32 \text{ pb} , \quad (36)$$

and for \mathcal{T}_b

$$\sigma_{\mathcal{T}_{b2} \rightarrow b, \bar{b}, \mu\bar{\mu}} \simeq \frac{3}{4} \sigma_{\mathcal{T}_{b0} \rightarrow b, \bar{b}, \mu\bar{\mu}} \simeq 7.2 \text{ fb} , \quad (37)$$

which, with the present integrated luminosity, should correspond to about 260 events.

However, the detection a tetra-bottom state in the channel $\mu\bar{\mu} b\bar{b}$ pair depends on the efficiency of the detection of a $b\bar{b}$ pair with an invariant mass of less than 1 GeV above threshold and with an average squared transverse momentum about 40 GeV^2 ⁶. The \mathcal{T} detection in this channel would be favorite if it were better than $2.7 \cdot 10^{-2}$. That is, the single beauty particle detection efficiency should be better than .16. This looks very difficult to reach considering the very low statistics of the production process.

Therefore we can conclude this analysis asserting that the most reliable channel where the tetra-bottom can be detected seem to be that of two $\mu\bar{\mu}$ pairs.

6 Conclusions.

The aim of this paper is to present a coherent and possibly complete description of the phenomenology of the compound states of heavy quarks, that is charm and bottom quarks. The paper is based on a non-relativistic quantum field theoretical approach to the dynamics and on the evaluation of the gluon-gluon luminosities at the 13 TeV LHC.

First of all, it must be remarked that the results should not be considered high precision results. This is due to four different factors. These are the relativistic corrections which are systematically disregarded, even for the charm flavor for which these corrections might be larger, and the poor knowledge of the parton-parton LHC luminosities in the region of interest, i.e.

⁶See footnote 2 and consider that the Quarkonium state $\Upsilon(4S)$, which mainly decays into a pair of beauty particles, has not been detected at the LHC.

between 3 and 20 GeV . Furthermore, we consider the production processes as purely collinear forgetting transverse momenta which are of the order of the particle masses, and we neglect higher order QCD perturbative corrections and hadronization corrections.

Some of these corrections should need very difficult calculations, some other are poorly known. Therefore, the reliability of our results should be limited to their order of magnitude. However, as it clearly appears from the experimental results on the charm tetra-quarks and quarkonia the experimental data suffer from uncertainties ranging from ten to fifty percent. This is mainly due to the production processes being very rare and the detection efficiencies very low in particular at the LHC.

In spite of these difficulties in the cases where a direct comparison of our results with the experimental data is possible, that is for the η_c production cross section, width and 2γ decay rate, our results are in reasonable, in one case even surprising, agreement with the experimental results. There is also agreement on the decay width of the η_b .

Concerning the recently uncovered tetra-charm at the LHCb a reasonable agreement exists for the data on the two $\mu\bar{\mu}$ pairs decay width and the ratio tetra-charm to double J/ψ production rates. However this agreement might be due to the poor quality of the present experimental data.

Therefore, despite the roughness of our approximations, we think useless to try to improve our calculations.

Our results on the tetra-bottom, which is the main purpose of the present paper, show the remarkable difficulty of the detection. As a matter of fact, the lack of the detection of the well-known η_b at the LHC and the fact that the production cross section of Υ pairs at the CMS is about two hundred times smaller than that of J/ψ pairs at the LHCb on a smaller rapidity interval gives a significant sign of the difficulty of the detection of any multi-bottom state. Our result for the ratio of the production cross section of a single tetra-bottom state $\sigma_{\mathcal{T}_b}$ at the CMS to that of the tetra-charm state $\sigma_{\mathcal{T}_c}$ at the LHCb, an amount which is about $4 \cdot 10^{-4}$, confirms the mentioned difficulty.

Thus, what we can do is try to single out the better detection channel. Considering that the hard version of the main decay channel is $b\bar{b} 2g$, that is, a pair of gluons together a $b\bar{b}$ pair, should correspond, after hadronization, to two gluon jets with total invariant mass near 10 GeV plus a pair of b-mesons near threshold ⁷ we think that one should have recourse to another decay channel due to the low selection efficiency of this channel. Note in particular that the detection efficiency of two gluon jets with total invariant mass of 10 GeV should be similar to that of the η_b which, according to our calculations, is produced at the CMS with a cross section of about one microbarn, and remains undetected after it has been reached an integrated luminosity of 36 fb^{-1} .

Therefore, we have considered the case where the gluon pair is replaced by a $\mu\bar{\mu}$ where the muon transverse momenta might reach six-seven GeV while that of the bottoms might be roughly the same of that in the $b\bar{b} 2g$ channel. From our calculations the branching ratio of the decay into this channel is $B_{\mathcal{T} \rightarrow b\bar{b}\mu\bar{\mu}} \sim 10^{-4}$, thus this channel is convenient if the selection efficiency of the pair of gluon jets mentioned above is worse than 10^{-4} .

The last possibility we have considered is the decay into two $\mu\bar{\mu}$ pairs, the channel in which

⁷And momentum difference of less than one GeV .

the tetra-charm has been detected at the LHCb [4] and the tetra-bottom has been looked for at the CMS [17] . In this channel the computed decay branching ratio is worth $B_{\mathcal{T} \rightarrow 2\mu 2\bar{\mu}} \sim 2 \cdot 10^{-5}$ and the resonant production cross section we have computed is about $\sigma_{\mathcal{T}_{b2} \rightarrow 2\mu 2\bar{\mu}} \simeq .18 \text{ fb}$. As mentioned in the previous Section this seems to be the favored channel for the tetra-bottom discovery because the detection efficiency of a $b\bar{b}$ pair near threshold is very low, however, before that, LHC has to reach an integrated luminosity of at least 500 fb^{-1} .

As a final comment we note that we have only discussed the results concerning \mathcal{T}_2 and \mathcal{T}_0 for which we have quoted the ratios of our results to the \mathcal{T}_2 ones. In particular we have forgotten the \mathcal{T}_1 state because, in our approximation , its production cross section vanishes at the LHC.

Appendices

A Interactions in the non-relativistic limit.

Beyond the evaluation of the production cross section of tetra-Quarks our work has been mainly devoted to the study of the properties of the Quarkonium and tetra-Quark states. We have used the same description of the tetra-Quark states already used in [5] and [6] assuming a non-relativistic structure based on the wave functions given in Eq.s (1) and (2) and on the fact that the Quarkonium radii D_c and D_b are sufficiently larger respectively of m_c^{-1} and m_b^{-1} . Since the energies of the light decay products are of the same order of magnitude of m_Q our non-relativistic choice is equivalent to assuming that the momenta of the initial Quarks might be neglected in the calculations of the transition amplitudes and hence the initial Quarks might be considered at rest in the reference system in which the tetra-Quark is almost at rest.

In the field operator which creates and destroys the non-relativistic Quarks the spinorial part does not depend on the momentum. Let us remind the structure of this field.

Choosing the γ matrices in the standard representation

$$\gamma_0 = \begin{pmatrix} 1 & 0 \\ 0 & -1 \end{pmatrix} \quad , \quad \gamma_i = \begin{pmatrix} 0 & -\sigma_i \\ \sigma_i & 0 \end{pmatrix} \quad , \quad \gamma_5 = \begin{pmatrix} 0 & 1 \\ 1 & 0 \end{pmatrix} \quad ,$$

we introduce the 4-component spinors

$$u_{\pm}(\vec{p}) = \begin{pmatrix} \sqrt{\frac{E+m}{2E}} \\ \frac{\vec{\sigma} \cdot \vec{p}}{\sqrt{2E(E+m)}} \end{pmatrix} w_{\pm} \quad , \quad v_{\pm}(\vec{p}) = \begin{pmatrix} \frac{\vec{\sigma} \cdot \vec{p}}{\sqrt{2E(E+m)}} \\ \sqrt{\frac{E+m}{2E}} \end{pmatrix} w_{\pm} \quad ,$$

where w is a two component spinor. More precisely

$$w_+ = \begin{pmatrix} 1 \\ 0 \end{pmatrix} \quad , \quad w_- = \begin{pmatrix} 0 \\ 1 \end{pmatrix} \quad .$$

Since the charge conjugation action is defined by $\psi^{(c)} = i\gamma_2 \psi^\dagger$ and since

$$i\gamma_2 u_{\pm}^*(\vec{p}) = \pm v_{\mp}(\vec{p}) \quad , \quad i\gamma_2 v_{\pm}^*(\vec{p}) = \mp v_{\mp}(\vec{p})$$

one has $a_{\pm}^{(c)}(\vec{p}) = b_{\pm}(\vec{p})$ e $b_{\pm}^{(c)}(\vec{p}) = a_{\pm}(\vec{p})$. Thus the fermionic field decomposes according

$$\psi(\vec{r}) = \frac{1}{(2\pi)^{\frac{3}{2}}} \int d\vec{p} \left(a_{\pm}(\vec{p}) u_{\pm}(\vec{p}) e^{i\vec{p} \cdot \vec{r}} \pm b_{\pm}^{\dagger}(\vec{p}) v_{\mp}(\vec{p}) e^{-i\vec{p} \cdot \vec{r}} \right).$$

In the non-relativistic limit, the momenta are negligible with respect to the Quark masses. Thus, the field becomes

$$\Psi(\vec{r}) = \frac{1}{(2\pi)^{\frac{3}{2}}} \int d\vec{p} \left(A_{\pm}(\vec{p}) U_{\pm} e^{i\vec{p} \cdot \vec{r}} \pm B_{\pm}^{\dagger}(\vec{p}) V_{\mp} e^{-i\vec{p} \cdot \vec{r}} \right) \equiv \tilde{A}_{\pm}(\vec{r}) U_{\pm} \pm \tilde{B}_{\pm}^{\dagger}(\vec{r}) V_{\mp}, \quad (38)$$

where $\tilde{A}(\vec{r})$ and $\tilde{B}(\vec{r})$ are the destruction operators in the point \vec{r} and the tetra-spinors are

$$U_{\pm} = \begin{pmatrix} w_{\pm} \\ 0 \end{pmatrix}, \quad V_{\pm} = \begin{pmatrix} 0 \\ w_{\pm} \end{pmatrix}.$$

Therefore we have

$$\pm V_{\mp} = -i\gamma_2 U_{\pm}, \quad \pm \bar{V}_{\mp} = i\bar{U}_{\pm} \gamma_2,$$

thus

$$\begin{aligned} \Psi(\vec{r}) &= [\tilde{A}_{\pm}(\vec{r}) - i\gamma_2 \tilde{B}_{\pm}^{\dagger}(\vec{r})] U_{\pm} = \int \frac{d\vec{p}}{(2\pi)^{\frac{3}{2}}} e^{i\vec{p} \cdot \vec{r}} [A_{\pm}(\vec{p}) - i\gamma_2 B_{\pm}^{\dagger}(-\vec{p})] U_{\pm}, \\ \bar{\Psi}(\vec{r}) &= \bar{U}_{\pm} [\tilde{A}_{\pm}^{\dagger}(\vec{r}) + i\gamma_2 \tilde{B}_{\pm}(\vec{r})] = \bar{U}_{\pm} \int \frac{d\vec{p}}{(2\pi)^{\frac{3}{2}}} e^{i\vec{p} \cdot \vec{r}} [A_{\pm}^{\dagger}(\vec{p}) + i\gamma_2 B_{\pm}(-\vec{p})]. \end{aligned} \quad (39)$$

Introducing the bilinear operator $(\bar{\Psi}(\vec{r}) \prod_i \gamma_{\mu_i} \Psi(\vec{r}))$ and selecting its destruction component we get

$$\left(\bar{\Psi}(\vec{r}) \prod_i \gamma_{\mu_i} \Psi(\vec{r}) \right) |_{distr} = i\tilde{B}_s(\vec{r}) \tilde{A}_{s'}(\vec{r}) (\bar{U}_s \gamma_2 \prod_i \gamma_{\mu_i} U_{s'})$$

which does not vanish in the non-relativistic limit only if the product of γ matrices contains an odd number of space component factors. After translation to the right-hand side the γ_0 factors one is left, up to a sign factor, with

$$\begin{aligned} \left(\bar{\Psi}(\vec{r}) \prod_i \gamma_{\mu_i} \Psi(\vec{r}) \right) |_{distr} &= i\tilde{B}_s(\vec{r}) \tilde{A}_{s'}(\vec{r}) (\bar{U}_s \gamma_2 \prod_{j=1}^{2n+1} \gamma_{l_j} U_{s'}) \\ &= i(-1)^{n+1} \tilde{B}_s(\vec{r}) \tilde{A}_{s'}(\vec{r}) (\sigma_2 \prod_{j=1}^{2n+1} \sigma_{l_j})_{ss'}, \end{aligned} \quad (40)$$

thus, for example, the destruction part of the space components of the current operator are given by

$$\left(\bar{\Psi}(\vec{r}) \gamma_i \Psi(\vec{r}) \right) |_{distr} = -i\tilde{B}_s(\vec{r}) \tilde{A}_{s'}(\vec{r}) (\sigma_2 \sigma_i)_{ss'},$$

and we have

$$\left(\bar{\Psi}(\vec{r}) \vec{V} \cdot \vec{\gamma} \Psi(\vec{r}) \right) |_{distr} = -i\tilde{B}_s(\vec{r}) \tilde{A}_{s'}(\vec{r}) (V)_{ss'}, \quad (41)$$

where

$$(V)_{ss'} \equiv \begin{pmatrix} V_y - iV_x & iV_z \\ iV_z & V_y + iV_x \end{pmatrix}_{ss'} \equiv \begin{pmatrix} -iV_+ & iV_z \\ iV_z & iV_- \end{pmatrix}_{ss'} . \quad (42)$$

The purpose of this Appendix consists in characterizing the effective Hamiltonians whose first order transition amplitude corresponds to those of processes whose invariant amplitudes are known.

With this aim we shall follow the formalism introduced in [7] from which one knows that, if $M_{f,i}$ is the invariant amplitude of a process with m particles in the initial state and n particles in the final state, the effective Hamiltonian for the same process must satisfy

$$\langle F | H_E | I \rangle = -(2\pi)^3 \delta(\vec{P}_F - \vec{P}_I) \frac{M_{f,i}}{\sqrt{\prod_{i=1}^{n+m} ((2\pi)^3 2E_i)}} . \quad (43)$$

If there appear non-relativistic fermions whose field is given in Eq. (39), the corresponding $\sqrt{2E_i}$ in the denominator must be omitted.

Thus, for example, to the first order in α , the effective Hamiltonian accounting for annihilation of a pair of heavy spinors (for example the Quarks $b\bar{b}$) at rest into a pair $\mu\bar{\mu}$ is given, neglecting the contribution of the exchange of a Z intermediate boson and summing over the Quark color, by

$$H_I = \frac{4\pi\alpha\zeta}{3s} \int d\vec{r} \left(\bar{\Psi}_a(\vec{r}) \gamma_\nu \Psi_a(\vec{r}) \right) (\bar{\psi}(\vec{r}) \gamma^\nu \psi(\vec{r})) \sim \frac{4\pi\alpha\zeta}{12m_Q^2} i \int d\vec{r} [\tilde{B}_{s,a}(\vec{r}) \tilde{A}_{s',a}(\vec{r}) j_{ss'}(\vec{r}) + h.c.] , \quad (44)$$

where s is the squared annihilation tetra-momentum, $h.c.$ stays for the terms containing heavy Quark creation operators, $\zeta = 1$ for the bottom and $\zeta = -2$ for the charm. We have set

$$j_\mu(\vec{r}) \equiv (\bar{\psi}(\vec{r}) \gamma_\mu \psi(\vec{r})) , \quad \text{and hence} , \quad \vec{j}(\vec{r}) \equiv (\bar{\psi}(\vec{r}) \vec{\gamma} \psi(\vec{r})) .$$

The field ψ may be a relativistic spinor field, for example that of the μ particle. In QCD where the light spinors are quarks and hence carry color, we shall introduce and sum over the color indices as in

$$j_\mu^\alpha(\vec{r}) \equiv t_{ab}^\alpha (\bar{\psi}_a(\vec{r}) \gamma_\mu \psi_b(\vec{r})) .$$

The Quark interaction Hamiltonian which has been used applying the variational method shown in the Introduction is

$$H_{int} = \alpha_S \int \frac{d\vec{r} d\vec{r}'}{4|\vec{r} - \vec{r}'|} (\delta_{da} \delta_{bc} - \frac{1}{3} \delta_{dc} \delta_{ba}) (A_{a\sigma}^\dagger(\vec{r}) A_{b\sigma}^\dagger(\vec{r}') - B_{b\sigma}^\dagger(\vec{r}) B_{a\sigma}(\vec{r}')) \\ (A_{c\sigma'}^\dagger(\vec{r}') A_{d\sigma'}^\dagger(\vec{r}) - B_{d\sigma'}^\dagger(\vec{r}') B_{c\sigma'}(\vec{r})) .$$

In the case of the first order in α annihilation of a pair $Q\bar{Q}$ with momenta $|\vec{p}| \ll m_b$ only the destruction Quark and anti-Quark operators, e.g. $\tilde{A}_{+,c}(\vec{r}) = \int d\vec{p} A_{+,c}(\vec{p}) \exp(i\vec{p} \cdot \vec{r}) / (2\pi)^{3/2}$, appear. Since the fields appearing in $\vec{j}(\vec{r})$ carry much larger momenta than (anti-)Quarks, it is possible to replace $\tilde{A}_{+,c}(\vec{r})$ with $\tilde{A}_{+,c}(\vec{0})$. Obviously the same holds true for the anti-Quark operator $\tilde{B}_{+,c}(\vec{r})$. As a consequence, the effective Hamiltonian may be written as

$$H_I \simeq \frac{\pi\alpha\zeta}{3 m_Q^2} i [\tilde{B}_{s,a}(\vec{0}) \tilde{A}_{s',a}(\vec{0}) \int d\vec{r} j_{ss'}(\vec{r}) + h.c.] . \quad (45)$$

Here, in Equation (44) and in the rest of this paper we shall only be interested in the part of the effective Hamiltonian which induces destruction of the heavy Quarks. Since we shall often deal with rather cumbersome formulae any, however limited, simplification will be appropriate. Therefore, in the following, we shall systematically omit any mention of the terms containing heavy Quark creation operators.

The same approximation will be systematically applied to the strong decays in the case of full annihilation of the heavy Quarks.

We add to the end of this Appendix few relations which will become useful in the case of full annihilation of the heavy Quarks. These are

$$\begin{aligned} < 0 | \tilde{B}_{s_2 l}(\vec{r}_2) \tilde{A}_{s_1 m}(\vec{r}_1) \tilde{B}_{s_4 n}(\vec{r}_4) \tilde{A}_{s_3 p}(\vec{r}_3) | \mathcal{T}_J, J_z, \vec{P} > = \Psi_{\mathcal{T}}(\vec{r}_1, \vec{r}_2, \vec{r}_3, \vec{r}_4, \vec{P}) \\ (\delta_{lp} \delta_{mn} - \delta_{np} \delta_{lm}) \Xi_{J, J_z}(s_i) , \end{aligned}$$

Noticing that, when the above operators act on the tetra-Quark states, that are color singlet states, the dependence of the result on the Quark color indices is independent of the state and hence the dependence of the matrix elements on the Quark color corresponds to a constant factor. Thus we can introduce the new notation

$$\tilde{B}_{s_2 l}(\vec{r}_2) \tilde{A}_{s_1 m}(\vec{r}_1) \tilde{B}_{s_4 n}(\vec{r}_4) \tilde{A}_{s_3 p}(\vec{r}_3) \equiv (\delta_{lp} \delta_{mn} - \delta_{np} \delta_{lm}) \tilde{B}_{s_2}(\vec{r}_2) \tilde{A}_{s_1}(\vec{r}_1) \tilde{B}_{s_4}(\vec{r}_4) \tilde{A}_{s_3}(\vec{r}_3) ,$$

hence, forgetting the Quark colors, we can introduce the further notation

$$< 0 | \tilde{B}_{s_2}(\vec{r}_2) \tilde{A}_{s_1}(\vec{r}_1) \tilde{B}_{s_4}(\vec{r}_4) \tilde{A}_{s_3}(\vec{r}_3) | \mathcal{T}_J, J_z, \vec{P} > = \Psi_{\mathcal{T}}(\vec{r}_1, \vec{r}_2, \vec{r}_3, \vec{r}_4, \vec{P}) \Xi_{J, J_z}(s_i) , \quad (46)$$

where

$$\begin{aligned} \Xi_0 &= \frac{1}{6} [2\delta_{s_2+} \delta_{s_1-} \delta_{s_4+} \delta_{s_3-} + 2\delta_{s_2-} \delta_{s_1+} \delta_{s_4-} \delta_{s_3+} - \delta_{s_2+} \delta_{s_1+} \delta_{s_4-} \delta_{s_3-} \\ &\quad - \delta_{s_2-} \delta_{s_1-} \delta_{s_4+} \delta_{s_3+} - \delta_{s_2+} \delta_{s_1-} \delta_{s_4-} \delta_{s_3+} - \delta_{s_2-} \delta_{s_1+} \delta_{s_4+} \delta_{s_3-}] , \\ \Xi_{1,1} &= \frac{1}{2\sqrt{3}} [\delta_{s_2-} \delta_{s_1+} \delta_{s_4+} \delta_{s_3+} + \delta_{s_2+} \delta_{s_1+} \delta_{s_4-} \delta_{s_3+} - \delta_{s_2+} \delta_{s_1-} \delta_{s_4+} \delta_{s_3+} \\ &\quad - \delta_{s_2+} \delta_{s_1+} \delta_{s_4+} \delta_{s_3-}] , \\ \Xi_{2,2} &= \frac{1}{\sqrt{3}} \delta_{s_2+} \delta_{s_1+} \delta_{s_4+} \delta_{s_3+} . \end{aligned} \quad (47)$$

For example, applying Eq. (46) we shall often compute

$$\begin{aligned} < 0 | B_{s_1 l}(\vec{P} + \frac{\vec{P}}{2}) A_{s_2 m}(\vec{P} - \frac{\vec{P}}{2}) \tilde{B}_{s_3 n}(\vec{0}) \tilde{A}_{s_4 p}(\vec{0}) | \mathcal{T}_J, J_z, \vec{P} > = (\delta_{lp} \delta_{mn} - \delta_{np} \delta_{lm}) \Xi_{J, J_z}(s_i) \\ \int \frac{d\vec{R} d\vec{r}}{(2\pi)^3} e^{-i(\vec{P} \cdot \vec{R} + \vec{P} \cdot \vec{r})} \Psi_{\mathcal{T}}(\vec{R} + \frac{\vec{r}}{2}, \vec{R} - \frac{\vec{r}}{2}, \vec{0}, \vec{0}, \vec{0}) = (\delta_{lp} \delta_{mn} - \delta_{np} \delta_{lm}) \Xi_{J, J_z}(s_i) \\ \frac{d^3 \delta^{\frac{3}{2}}}{\pi^{\frac{15}{4}} (d^2 + 2\delta^2)^{\frac{3}{2}}} e^{-[2 \frac{d^2 \delta^2}{d^2 + 2\delta^2} p^2 + \frac{d^2}{4} P^2]} . \end{aligned} \quad (48)$$

In practice, computing the matrix elements of the effective Hamiltonian for the decay of a tetra-Quarks, the matrix elements shall be divided in two factors using the factorization of the

Fock space in a non-relativistic part containing the heavy Quark states and in a relativistic part spanned by the light particle states.

The first step of the calculation will consist in computing the operator valued matrix element $\langle H \rangle_{NR}$ of the effective Hamiltonian between the initial state of the tetra-Quark and the heavy Quark component of the final state. The resulting $\langle H \rangle_{NR}$ will be an operator in the Fock space of the light particles. The second step will consist in the calculation of the c-number matrix element of $\langle H \rangle_{NR}$ between the vacuum state and the final state of the light particles.

B The electromagnetic decays

The simplest test of our scheme consists in the comparison of the decay rates of the η_Q 's into two gammas. This decay is induced by the effective Hamiltonian whose bottom destruction component is

$$H_{2\gamma} = -i \frac{\pi \alpha \zeta^2}{9 m_Q} \tilde{B}_{sa}(\vec{0}) \tilde{A}_{s'a}(\vec{0}) \sum_{\lambda} [\lambda (\sigma_2)_{ss'} + (\sigma_2 \vec{\sigma} \cdot \vec{v})_{ss'}] \int \frac{d\vec{q}}{q} a_{\lambda}^{\dagger}(\vec{q}) a_{\lambda}^{\dagger}(-\vec{q}) .$$

The corresponding transition matrix element is

$$\langle 0 | a_{\lambda_1}(\vec{q}_1) a_{\lambda_2}(\vec{q}_2) H_{2\gamma} | \eta_Q, \vec{0} \rangle = -i \frac{\alpha \zeta^2}{3^{\frac{3}{2}} \pi^{\frac{5}{4}} m_Q D_Q^{\frac{3}{2}}} \delta_{\lambda_1 \lambda_2} \lambda_1 \frac{\delta(\vec{k}_1 + \vec{k}_2)}{k_1} ,$$

and the decay rate into two gammas is given by

$$\Gamma_{\eta_Q \rightarrow 2\gamma} = \frac{4 \alpha^2 \zeta^4}{3^3 \sqrt{\pi} m_Q^2 D_Q^3} . \quad (49)$$

B.1 The decay $\mathcal{T} \rightarrow \mu \bar{\mu} \mathcal{Q}$.

Here we compute the decay rate of the state \mathcal{T}_2 into two $\mu \bar{\mu}$ pairs assuming a two step process [17], in the first step \mathcal{T}_2 decays electromagnetically into a $\mu \bar{\mu}$ pair and a Quarkonium state \mathcal{Q} , in the second step \mathcal{Q} decays into another $\mu \bar{\mu}$ pair.

Let us thus consider the matrix element of the effective Hamiltonian given in Eq. (45) between the initial state of \mathcal{T}_2 at rest and a final Quarkonium \mathcal{Q} state. The corresponding Fock vector states are given by $|\mathcal{T}_2, 2, \vec{0}\rangle$ shown in Eq. (10) and the Quarkonium state $|\mathcal{Q}, 1, \vec{P}\rangle$ given in Eq. (5).

In this first example we show the computation strategy that we shall apply many times in the following and is anticipated in Appendix A.

Considering the first of the two steps of the already discussed procedure we shall use the effective Hamiltonian given in Eq. (45) together with Eq. s (46), (47) and (41) with

$$V = j_i(\vec{r}) = (\bar{\psi}_{\mu}(\vec{r}) \gamma_i \psi_{\mu}(\vec{r})) ,$$

obtaining the operator in the muon Fock space

$$\begin{aligned}
\langle \mathcal{Q}, 1, \vec{P} | H_I | \mathcal{T}_2, 2, \vec{0} \rangle_{NR} &\sim i \frac{\pi \alpha \zeta}{3^{\frac{3}{2}} m_b^2} \int \prod_{j=1}^2 d\vec{\rho}_j \int d\vec{R} \Psi_{\mathcal{Q}}^*(\vec{\rho}_1, \vec{\rho}_2, \vec{P}) \Psi_{\mathcal{T}}(\vec{\rho}_1, \vec{\rho}_2, \vec{0}, \vec{0}, \vec{0}) (\delta_{cd} \delta_{cd} \\
&- \delta_{cc} \delta_{dd}) \Xi_0(+, +, s, s') j_{ss'} = \frac{-i \alpha \zeta 2^{\frac{5}{2}} D^{\frac{3}{2}} d^3 \delta^{\frac{3}{2}}}{3 \pi^2 (4\delta^2 d^2 + D^2(d^2 + 2\delta^2))^{\frac{3}{2}} m_b^2} e^{-\frac{P^2 d^2}{4}} \int d\vec{r} j_+(\vec{r}) e^{-i\vec{P} \cdot \vec{r}} \\
&.
\end{aligned} \tag{50}$$

Then the second step computing the transition matrix element in the muon Fock space is

$$\begin{aligned}
\langle \mathcal{Q}, 1, \vec{P}, \vec{k}_1, \lambda_1, \vec{k}_2, \lambda_2 | H_I | \mathcal{T}_2, 2, \vec{0} \rangle &= \frac{-i \alpha 2^{\frac{3}{2}} D^{\frac{3}{2}} d^3 \delta^{\frac{3}{2}}}{3 \pi^2 (4\delta^2 d^2 + D^2(d^2 + 2\delta^2))^{\frac{3}{2}} m_Q^2 \sqrt{k_1 k_2}} e^{-\frac{P^2 d^2}{4}} \\
&(\bar{u}_{\lambda_1}(\vec{k}_1) \gamma_+ v_{\lambda_2}(\vec{k}_2)) \delta(\vec{k}_1 + \vec{k}_2) .
\end{aligned}$$

Therefore the decay rate of the \mathcal{T}_2 at rest into $\mathcal{Q}\mu\bar{\mu}$ is given by

$$\begin{aligned}
\Gamma_{\mathcal{T}_2 \rightarrow \mathcal{Q}\mu\bar{\mu}} &\sim \frac{2^{\frac{23}{2}} \alpha^2 \zeta^2 d^3 \delta^3 D^3}{27 \sqrt{\pi} (4d^2 \delta^2 + D^2(d^2 + 2\delta^2))^3 m_Q^2} \\
&\sim \frac{2^{\frac{19}{2}} d^3 \delta^3 D^6}{3(4d^2 \delta^2 + D^2(d^2 + 2\delta^2))^3} \Gamma_{\mathcal{Q} \rightarrow \mu\bar{\mu}}
\end{aligned} \tag{51}$$

Note that the final result depends on the Quark charge only through $\Gamma_{\mathcal{Q} \rightarrow \mu\bar{\mu}}$.

The decay rate of the \mathcal{T}_0 is easily computed following the same procedure and introducing a factor 3 taking into account the spin degeneracy of the final \mathcal{Q} . Therefore we have

$$\Gamma_{\mathcal{T}_0 \rightarrow \mathcal{Q}\mu\bar{\mu}} \sim \frac{2^{\frac{15}{2}} d^3 \delta^3 D^6}{3(4d^2 \delta^2 + D^2(d^2 + 2\delta^2))^3} \Gamma_{\mathcal{Q} \rightarrow \mu\bar{\mu}} \simeq \frac{1}{4} \Gamma_{\mathcal{T}_2 \rightarrow \mathcal{Q}\mu\bar{\mu}} \tag{52}$$

The transition rate $\mathcal{T}_1 \rightarrow \mathcal{Q}\mu\bar{\mu}$ vanishes due to charge conjugation invariance.

Now the decay rate into two $\mu\bar{\mu}$ pairs is easily computed multiplying the above results by the \mathcal{Q} branching fraction into a $\mu\bar{\mu}$ pair. We get

$$\begin{aligned}
\Gamma_{\mathcal{T}_2 \rightarrow 2\mu\bar{\mu}} &= 4\Gamma_{\mathcal{T}_0 \rightarrow 2\mu\bar{\mu}} = \frac{2^{\frac{19}{2}} d^3 \delta^3 D^6}{3(4d^2 \delta^2 + D^2(d^2 + 2\delta^2))^3} \frac{\Gamma_{\mathcal{Q} \rightarrow \mu\bar{\mu}}^2}{\Gamma_{\mathcal{Q}}} \\
&\simeq 240 \frac{d^3 \delta^3 D^6}{(4d^2 \delta^2 + D^2(d^2 + 2\delta^2))^3} \frac{\Gamma_{\mathcal{Q} \rightarrow \mu\bar{\mu}}^2}{\Gamma_{\mathcal{Q}}} .
\end{aligned} \tag{53}$$

B.2 The decay $\mathcal{T} \rightarrow \mu\bar{\mu}Q\bar{Q}$.

Then we consider the electromagnetic tetra-Quark decay into an open $Q\bar{Q}$ pair and a $\mu\bar{\mu}$ pair. We have suggested in the Conclusions Chapter that the decay into this channel might be interesting for the tetra-Quark detection.

The calculation of the decay rate $\mathcal{T} \rightarrow \mu\bar{\mu}Q\bar{Q}$ is analogous to that in the final channel $\mathcal{Q}\mu\bar{\mu}$. One must replace the Quarkonium wave function by the product of two plane waves.

Thus beginning with \mathcal{T}_2 , let us consider the production of a $\mu\bar{\mu}$ and $Q\bar{Q}$ pairs. Using the variables $\vec{\rho} = \vec{\rho}_1 - \vec{\rho}_2$, $\vec{r} = (\vec{\rho}_1 + \vec{\rho}_2)/2$ and $\vec{P} = \vec{p}_1 + \vec{p}_2$ together with $\vec{p} = (\vec{p}_1 + \vec{p}_2)/2$, in analogy with Eq. (50) we get

$$\begin{aligned} < 0 | B_{s_1 c}(\vec{p}_1), A_{s_2 d}(\vec{p}_2), \beta \lambda_1(\vec{k}_1), \alpha \lambda_2(\vec{k}_2) | H_I | \mathcal{T}_2, 2, \vec{0} > \sim \frac{-i 2 \alpha \zeta \delta_{s_1 + \delta_{s_2} + \delta_{cd}} d^3 \delta^{\frac{3}{2}}}{3^{\frac{3}{2}} \pi^{\frac{11}{4}} m_b^2 (d^2 + 2\delta^2)^{\frac{3}{2}}} \\ \int d\vec{r} < \vec{k}_1, \lambda_1, \vec{k}_2, \lambda_2 | j_+(\vec{r}) | 0 > e^{-(2p^2 \frac{\delta^2}{d^2 + 2\delta^2} + \frac{P^2 d^2}{4})} , \end{aligned} \quad (54)$$

from which we have the decay rate

$$\Gamma_{\mathcal{T}_2 \rightarrow Q, \bar{Q}, \mu\bar{\mu}} \simeq \frac{\alpha^2 \zeta^2 2^{\frac{11}{2}}}{3^3 \sqrt{\pi} m_b^2 (d^2 + 2\delta^2)^{\frac{3}{2}}} \simeq .95 \frac{\alpha^2 \zeta^2}{m_Q^2 (d^2 + 2\delta^2)^{\frac{3}{2}}} . \quad (55)$$

Using Eq. (47) in Appendix A it is easy to see that

$$\Gamma_{\mathcal{T}_0 \rightarrow Q, \bar{Q}, \mu\bar{\mu}} = \frac{1}{4} \Gamma_{\mathcal{T}_2 \rightarrow Q, \bar{Q}, \mu\bar{\mu}} . \quad (56)$$

C The second order in α_S .

Now we consider the effective Hamiltonian for the second order in α_S annihilations of a $Q\bar{Q}$ pair in non-relativistic movement in either a gluon pair, or a light $q\bar{q}$ pair. These correspond to the diagrams ⁸ shown in Figure 1.

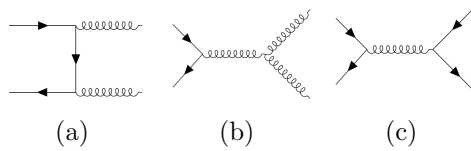


Figure 1: The order α_S^2

In the reference frame in which the initial heavy Quarks are in non-relativistic movement we can set $|\vec{p}| \sim |\vec{p}'| \ll |\vec{q}| \sim |\vec{q}'| \sim m_Q$ identifying the four-vectors

$$p \sim p' \sim m_Q \begin{pmatrix} 0 \\ 1 \end{pmatrix} , \quad q \sim m_Q \begin{pmatrix} \vec{v} \\ 1 \end{pmatrix} , \quad q' \sim m_Q \begin{pmatrix} -\vec{v} \\ 1 \end{pmatrix} , \quad q - p \sim p - q' \sim m_Q \begin{pmatrix} \vec{v} \\ 0 \end{pmatrix} , \quad (57)$$

⁸Computing the effective Hamiltonian corresponding to a Feynman diagram we have to replace the external lines by the corresponding field operators. This changes the nature of the diagrams because the effective Hamiltonian matrix element corresponding to single diagram contains as many different terms as there are permutations of identical particles both in the initial and the final state. For example, in the scalar theory the first order invariant transition amplitude of two particles in two particles is just the coupling constant λ . On the contrary the effective Hamiltonian is just the first order interaction operator $\int d\vec{r} \lambda \phi^4(\vec{r})/4!$.

where the unimodular three-vector \vec{v} is orthogonal to the polarization three-vectors $\vec{\epsilon}_\lambda(\vec{q})$ e $\vec{\epsilon}_{\lambda'}(\vec{q}')$. Choosing $\vec{\epsilon}_\lambda(-\vec{q}) = \vec{\epsilon}_\lambda^*(\vec{q})$ and setting $\vec{\epsilon}_\lambda(\vec{q}) = (\vec{x} + i\lambda\vec{y})/\sqrt{2}$ ⁹, if \vec{q} is parallel to the z axis, we have

$$i\vec{v} \cdot (\vec{\epsilon}_{\lambda'}^*(\vec{q}') \wedge \vec{\epsilon}_\lambda^*(\vec{q})) = \lambda\delta_{\lambda\lambda'} \quad , \quad \vec{\epsilon}_{\lambda'}^*(\vec{q}') \cdot \vec{\epsilon}_\lambda^*(\vec{q}) = \delta_{\lambda\lambda'} \quad . \quad (58)$$

Note that above and in the following p e q denote momentum four-vectors. However, we also use, e.g. q to denote the energy of a massless particle. We believe that this choice is not confusing while it remarkably simplifies our notation.

Now it is worth using the following identities which follow from Eq. (40)

$$\begin{aligned} \bar{U}_{s'}\gamma_2\gamma_0\gamma_5 U_s &= (\sigma_2)_{s's} \quad , \quad \bar{U}_{s'}\gamma_2\gamma_i U_s = -(\sigma_2\sigma_i)_{s's} \quad , \\ \bar{U}_{s'}\gamma_2\gamma_i\gamma_j\gamma_k U_s &= \delta_{ij}(\sigma_2\sigma_k)_{s's} + \delta_{jk}(\sigma_2\sigma_i)_{s's} - \delta_{ik}(\sigma_2\sigma_j)_{s's} + i\epsilon_{ijk}(\sigma_2)_{s's} \quad , \end{aligned} \quad (59)$$

and the well-known $SU(3)$ identity

$$(t^\alpha t^\beta)_{ab} = \frac{1}{2}[(d^{\alpha\beta\gamma} + if^{\alpha\beta\gamma}t_{ab}^\gamma + \frac{1}{3}\delta^{\alpha\beta}\delta_{ab}] \quad . \quad (60)$$

Using the simplifications, already applied to H_I given in Eq.s (45), (39) and (40), we have the effective Hamiltonian for the destruction processes of two heavy Quarks and the creation of light particles

$$\begin{aligned} H_{2l} = & -i\frac{\pi}{2}\frac{\alpha_S}{m_Q}\tilde{B}_{sa}(\vec{0})\tilde{A}_{s'b}(\vec{0})\left[\int\frac{d\vec{q}}{q}a_{\lambda\alpha}^\dagger(\vec{q})a_{\lambda\beta}^\dagger(-\vec{q})[3i(\sigma_2\vec{\sigma}\cdot\vec{v})_{ss'}f^{\alpha\beta\gamma}t_{ab}^\gamma\right. \\ & \left. + \lambda(\sigma_2)_{ss'}(d^{\alpha\beta\gamma}t_{ab}^\gamma + \frac{\delta^{\alpha\beta}\delta_{ab}}{3})\right] + \frac{2}{m_Q}t_{ab}^\alpha\int d\vec{r}(\sigma_2\vec{\sigma}\cdot\vec{j})_{ss'}^\alpha(\vec{r}) \quad , \end{aligned} \quad (61)$$

where $a_{\alpha\lambda}(\vec{q})$ is the destruction operator of a gluon with helicity λ and color α . The four vectors $\epsilon_\lambda(\vec{q})$ e $\epsilon_{\lambda'}(\vec{q}')$ are purely space-like physical polarization vectors.

The decay amplitude of η_Q into two gluons corresponds to diagram (a) which leads to the matrix element

$$\langle 0|a_{\lambda_1,\gamma}(\vec{q}_1)a_{\lambda_2,\delta}(\vec{q}_2)|H_{2l}|\eta_Q,\vec{0}\rangle = i\frac{\alpha_S\lambda_1\delta_{\lambda_1\lambda_2}\delta^{\gamma\delta}}{2\sqrt{3}\pi^{\frac{5}{4}}D_Q^{\frac{3}{2}}m_Q}\frac{\delta(\vec{q}_1+\vec{q}_2)}{q_1} \quad , \quad (62)$$

from which one has the decay rate

$$\Gamma_{\eta_Q\rightarrow 2g} = \frac{8\alpha_s^2(m_Q^2)}{3\sqrt{\pi}m_Q^2D_Q^3} \quad . \quad (63)$$

If the full width of η_Q were due to the decay into two gluons, setting $\alpha_S(m_c^2) = .32$ and $\alpha_S(m_b^2) = .2$ we should have $\Gamma_{\eta_c} \simeq 16 \text{ MeV}$ and $\Gamma_{\eta_b} \simeq 5.3 \text{ MeV}$. It is apparent that our results are compatible with the widths given by the Particle Data Books. Furthermore, the third order contributions should not give substantial corrections.

⁹Where \vec{x} and \vec{y} are also unimodular and parallel to the corresponding axes.

It is also easy to compute the rate of the decay $\mathcal{T}_2 \rightarrow Q\bar{Q}2g$ which is determined at the second order by the matrix element

$$\begin{aligned} < 0 | a_{\lambda_1, \gamma}(\vec{q}_1) a_{\lambda_2, \delta}(\vec{q}_2) B_{s_1 l}(\vec{P} + \frac{\vec{p}}{2}) A_{s_2 m}(\vec{P} - \frac{\vec{p}}{2}) | H_{2l} | \mathcal{T}_2, 2, \vec{0} > = -i \frac{\sqrt{3} \alpha_S d^3 \delta^{\frac{3}{2}}}{\pi^{\frac{11}{4}} (d^2 + 2\delta^2)^{\frac{3}{2}} m_Q^2} \\ \delta_{\lambda_1 \lambda_2} f^{\gamma \delta \tau} t_{lm}^{\tau} \delta(\vec{q}_1 + \vec{q}_2) v_+ e^{-[2 \frac{d^2 \delta^2}{d^2 + 2\delta^2} p^2 + \frac{d^2}{4} P^2]}, \end{aligned}$$

where $\vec{v} \equiv \vec{q}_1/q_1$. Thence the decay rate $\mathcal{T}_2 \rightarrow Q\bar{Q}2g$ turns out to be

$$\Gamma_{\mathcal{T}_2 \rightarrow Q\bar{Q}2g} = \frac{48 \alpha_S^2}{\sqrt{2\pi} m_Q^2 (d^2 + 2\delta^2)^{\frac{3}{2}}} \simeq 19 \frac{\alpha_S^2}{m_Q^2 (d^2 + 2\delta^2)^{\frac{3}{2}}}. \quad (64)$$

Moving to the decay $\mathcal{T}_2 \rightarrow Q\bar{Q}q\bar{q}$ whose amplitude is given by the matrix element

$$\begin{aligned} < 0 | \beta_{h_1, f}(\vec{k}_1) \alpha_{h_2, g}(\vec{k}_2) B_{s_1 l}(\vec{P} + \frac{\vec{p}}{2}) A_{s_2 m}(\vec{P} - \frac{\vec{p}}{2}) | H_{2l} | \mathcal{T}_2, 2, \vec{0} > = -\frac{\delta(\vec{k}_1 + \vec{k}_2)}{k_1} \delta_{s_1 + \delta_{s_2 +}} \\ \frac{\alpha_S d^3 \delta^{\frac{3}{2}}}{\sqrt{3} \pi^{\frac{11}{4}} (d^2 + 2\delta^2)^{\frac{3}{2}} 4 m_Q^2} (\delta_{lg} \delta_{fm} - \frac{1}{3} \delta_{fg} \delta_{lm}) \bar{u}_{h'}(-\vec{k}_1) \gamma_+ v_h(\vec{k}_1) e^{-[2 \frac{d^2 \delta^2}{d^2 + 2\delta^2} p^2 + \frac{d^2}{4} P^2]}, \end{aligned}$$

we get the decay rate

$$\Gamma_{\mathcal{T}_2 \rightarrow Q\bar{Q}q\bar{q}} = \frac{2^5 \alpha_S^2}{9 \sqrt{2\pi} m_b^2 (d^2 + 2\delta^2)^{\frac{3}{2}}}. \quad (65)$$

The sum of the two rates gives

$$\Gamma_{\mathcal{T}_2} \simeq \frac{20 \alpha_S^2}{m_Q^2 (d^2 + 2\delta^2)^{\frac{3}{2}}}, \quad (66)$$

If instead we consider the rate of the decay $\mathcal{T}_0 \rightarrow Q\bar{Q}2g$ whose amplitude is given by the matrix element

$$\begin{aligned} < 0 | a_{\lambda_1, \gamma}(\vec{q}_1) a_{\lambda_2, \delta}(\vec{q}_2) B_{s_1 l}(\vec{P} + \frac{\vec{p}}{2}) A_{s_2 m}(\vec{P} - \frac{\vec{p}}{2}) | H_{2l} | \mathcal{T}_0, \vec{0} > = \frac{\alpha_S d^3 \delta^{\frac{3}{2}}}{2 \pi^{\frac{11}{4}} (d^2 + 2\delta^2)^{\frac{3}{2}} m_Q^2} \\ \delta(\vec{q}_1 + \vec{q}_2) \delta_{\lambda_1 \lambda_2} \left[f^{\gamma \delta \tau} t_{lm}^{\tau} (v_z (\delta_{s_1, +} \delta_{s_2, -} + \delta_{s_1, +} \delta_{s_2, -}) - v_- \delta_{s_1, +} \delta_{s_2, +} + v_+ \delta_{s_1, -} \delta_{s_2, -}) \right. \\ \left. - \lambda_1 (d^{\gamma \delta \tau} t_{lm}^{\tau} - \frac{1}{3} \delta^{\gamma \delta} \delta_{lm}) (\delta_{s_1, -} \delta_{s_2, +} - \delta_{s_1, +} \delta_{s_2, -}) \right] e^{-[2 \frac{d^2 \delta^2}{d^2 + 2\delta^2} p^2 + \frac{d^2}{4} P^2]}, \end{aligned}$$

we find the decay rate

$$\Gamma_{\mathcal{T}_0 \rightarrow Q\bar{Q}2g} = \frac{64 \alpha_S^2}{3\sqrt{2\pi} m_Q^2 (d^2 + 2\delta^2)^{\frac{3}{2}}} \simeq 8.6 \frac{\alpha_S^2}{m_Q^2 (d^2 + 2\delta^2)^{\frac{3}{2}}}. \quad (67)$$

On the contrary the amplitude of the decay $\mathcal{T}_0 \rightarrow Q\bar{Q}q\bar{q}$ is determined by the matrix element

$$\begin{aligned} < 0 | \beta_{h_1, f}(\vec{k}_1) \alpha_{h_2, g}(\vec{k}_2) B_{s_1 l}(\vec{P} + \frac{\vec{P}}{2}) A_{s_2 m}(\vec{P} - \frac{\vec{P}}{2}) | H_{2l} | \mathcal{T}_0, \vec{0} > = - \frac{\alpha_S d^3 \delta^{\frac{3}{2}}}{24 \pi^{\frac{11}{4}} (d^2 + 2\delta^2)^{\frac{3}{2}} m_Q^2} \\ & (\delta_{lf} \delta_{gm} - \frac{1}{3} \delta_{fg} \delta_{lm}) \frac{\delta(\vec{k}_1 + \vec{k}_2)}{k_1} \bar{u}_{h_1 g}(\vec{k}_1) [\delta_{s_1 - \delta_{s_2 -}} (\gamma_x + i\gamma_y) - \delta_{s_1 + \delta_{s_2 +}} (\gamma_x - i\gamma_y) \\ & + (\delta_{s_1 + \delta_{s_2 -}} + \delta_{s_1 - \delta_{s_2 +}}) \gamma_z] v_{h_2 f}(-\vec{k}_1) e^{-[2 \frac{d^2 \delta^2}{d^2 + 2\delta^2} p^2 + \frac{d^2}{4} P^2]}. \end{aligned}$$

Thus the rate of the decay $\mathcal{T}_0 \rightarrow Q\bar{Q}q\bar{q}$ is

$$\Gamma_{\mathcal{T}_0 \rightarrow Q\bar{Q}q\bar{q}} = \frac{8 \alpha_S^2}{9 \sqrt{2\pi} m_Q^2 (d^2 + 2\delta^2)^{\frac{3}{2}}} \simeq 0.35 \frac{\alpha_S^2}{m_Q^2 (d^2 + 2\delta^2)^{\frac{3}{2}}}. \quad (68)$$

Summing the two contributions to the second order decay rate we get

$$\Gamma_{\mathcal{T}_0} \simeq 9 \frac{\alpha_S^2}{m_Q^2 (d^2 + 2\delta^2)^{\frac{3}{2}}}, \quad (69)$$

which is roughly half of the second order decay rate of \mathcal{T}_2 .

D Tetra-Quark transition to a pair of light particles at the order α_S^4 .

Postponing to a further paper the study of the third order QCD transitions, now we discuss the transition amplitudes of a Tetra-Quark into a pair of light particles. This choice is justified in Chapter 4 where we have discussed the Drell-Yan mechanism. We have seen that the \mathcal{T} production is due to a two parton fusion and that the case of two gluons is favored with respect to that of a light $q\bar{q}$ pair. Both are a fourth order processes.

D.1 The transition $\mathcal{T} \leftrightarrow 2g$ to two gluons.

We begin with the transition to two gluons which corresponds to the above diagrams. Figure 2 shows ten diagrams corresponding to ten terms of the effective Hamiltonian that we compute in the order. For each term we compute the action of the four Quark destruction part on the state of a \mathcal{T} at rest.

In the calculation we label by 1 and 3 the initial Quarks and by 2 and 4 the initial anti-Quarks.

We must take into account that

1) Since the initial state is a color singlet there always appears the color factor $\delta_{c_1 c_4} \delta_{c_2 c_3} - \delta_{c_1 c_2} \delta_{c_3 c_4}$ which is implicitly taken into account.

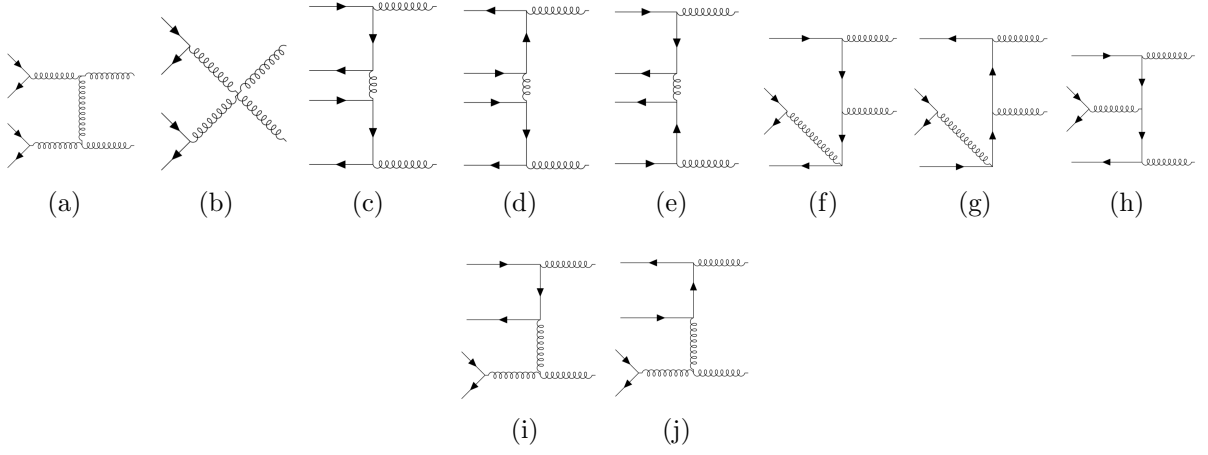


Figure 2: The transition $\mathcal{T} \leftrightarrow 2g$.

2) We shall choose the polarization vectors $\epsilon_\lambda(\vec{q})$ as in Appendix B. Simplifying the notation we shall omit their complex conjugation foreseen for the creation part of the gluon field.

3) We shall neglect the three-momenta of the Quarks while the four-momenta of the gluons and Quarks will be chosen as they are in Equation (57).

We introduce the two gluon creation operator

$$\int \frac{d\vec{q}}{2q} a_{\lambda\alpha}^\dagger(\vec{q}) a_{\lambda'\beta}^\dagger(-\vec{q}) \equiv \Xi_{\alpha\beta\lambda\lambda'} \quad , \quad \delta_{\alpha\beta} \Xi_{\alpha\beta\lambda\lambda'} \equiv \Xi_{\lambda\lambda'} \quad .$$

We begin from the **diagram a** for which, using Eq.s (40), (41), (42), (46) and (47) and introducing the further simplified notation

$$\epsilon_\lambda(\vec{q}) \equiv \epsilon \quad , \quad \epsilon_{\lambda'}(-\vec{q}) \equiv \epsilon' \quad ,$$

we have,¹⁰

$$\begin{aligned} H_a \sim & \frac{3 g^4 \Xi_{\alpha\beta\lambda\lambda'}}{2(2m_Q)^6} \epsilon_{\lambda\eta}(\vec{q}) \epsilon_{\lambda'\tau}(-\vec{q}) (g^{\eta\xi} 2(q-p)^\mu - g^{\eta\mu} (2p+q)^\xi) (-g^{\nu\tau} (2p+q')^\xi) \\ & + g^{\tau\xi} 2(p+q')^\nu (\bar{\Psi}_2(\vec{0}) \gamma_\mu \Psi_1(\vec{0})) (\bar{\Psi}_4(\vec{0}) \gamma_\nu \Psi_3(\vec{0})) = -\frac{3 g^4 \Xi_{\lambda\lambda'}}{2(2m_Q)^4} \tilde{B}_{s_2}(0) \tilde{A}_{s_1}(0) \\ & \tilde{B}_{s_4}(0) \tilde{A}_{s_3}(0) [5(\sigma_2 \vec{\sigma} \cdot \vec{\epsilon})_{s_2 s_1} (\sigma_2 \vec{\sigma} \cdot \vec{\epsilon}')_{s_4 s_3} + 4(\vec{\epsilon} \cdot \vec{\epsilon}') (\sigma_2 \vec{\sigma} \cdot \vec{v})_{s_2 s_1} (\sigma_2 \vec{\sigma} \cdot \vec{v})_{s_4 s_3}] \quad . \end{aligned}$$

Passing to the **diagram b** and using again Eq.s (40), (41), (42), (46) and (47), we have

$$\begin{aligned} H_b \sim & -\frac{g^4 \Xi_{\alpha\beta\lambda\lambda'}}{(2m_Q)^4} Tr(t^\gamma t^\delta) f^{\alpha\gamma\sigma} f^{\beta\delta\sigma} (\bar{\Psi}_2(\vec{0}) \gamma_\sigma \Psi_1(\vec{0})) (\bar{\Psi}_4(\vec{0}) \gamma_\rho \Psi_3(\vec{0})) \epsilon_{\lambda\mu}(\vec{q}) \epsilon_{\lambda'\nu}(-\vec{q}) \\ & (2g^{\mu\nu} g^{\rho\sigma} - g^{\mu\sigma} g^{\nu\rho} - g^{\mu\rho} g^{\nu\sigma}) = 3 \frac{g^4 \Xi_{\lambda\lambda'}}{(2m_Q)^4} \tilde{B}_{s_2}(0) \tilde{A}_{s_1}(0) \tilde{B}_{s_4}(0) \tilde{A}_{s_3}(0) \\ & [\vec{\epsilon} \cdot \vec{\epsilon}' (\sigma_2 \vec{\sigma}_i)_{s_2 s_1} (\sigma_2 \vec{\sigma}_i)_{s_4 s_3} - (\sigma_2 \vec{\epsilon} \cdot \vec{\sigma})_{s_2 s_1} (\sigma_2 \vec{\epsilon}' \cdot \vec{\sigma})_{s_4 s_3}] \quad . \end{aligned}$$

¹⁰Remember that we disregard the part of the effective Hamiltonian which contains Quark or anti-Quark creation operators.

For the **diagram c**, considering the invariance of the operator Ξ under the two gluon creation operators exchange, that is under $\epsilon \leftrightarrow \epsilon'$ and $\vec{v} \leftrightarrow -\vec{v}$, we have

$$\begin{aligned} H_c &\sim -\frac{g^4 \Xi_{\alpha\beta\lambda\lambda'}}{(2m_Q)^6} (\bar{\Psi}_2(\vec{0})\gamma^\rho(\not{p} - \not{q} + m_Q)\not{\epsilon}_\lambda(\vec{q})\Psi_1(\vec{0}))(\bar{\Psi}_4(\vec{0})\not{\epsilon}_{\lambda'}(-\vec{q})(\not{q}' - \not{p} + m_Q) \\ &\gamma_\rho\Psi_3(\vec{0}))[Tr(t^\alpha t^\gamma t^\beta t^\gamma) - Tr(t^\alpha t^\gamma)Tr(t^\gamma t^\beta)] = -\frac{5}{12} \frac{g^4 \Xi_{\lambda\lambda'}}{(2m_Q)^4} \tilde{B}_{s_2}(0)\tilde{A}_{s_1}(0)\tilde{B}_{s_4}(0)\tilde{A}_{s_3}(0) \\ &[2(\sigma_2\vec{\sigma} \cdot \vec{\epsilon})_{s_2s_1}(\sigma_2\vec{\sigma} \cdot \vec{\epsilon}')_{s_4s_3} + (\vec{\epsilon} \cdot \vec{\epsilon}')[(\sigma_2\vec{\sigma} \cdot \vec{v})_{s_2s_1}(\sigma_2\vec{\sigma} \cdot \vec{v})_{s_4s_3} + (\sigma_2)_{s_2s_1}(\sigma_2)_{s_4s_3}]] \ . \end{aligned}$$

Passing to the **diagram d** we have

$$\begin{aligned} H_d &\sim -\frac{g^4 \Xi_{\alpha\beta\lambda\lambda'}}{(2m_Q)^6} (\bar{\Psi}_2(\vec{0})\gamma^\rho(\not{p} - \not{q} + m_Q)\not{\epsilon}_\lambda(\vec{q})\Psi_1(\vec{0})) (\bar{\Psi}_4(\vec{0})\gamma_\rho(\not{p} - \not{q}' + m_Q)\not{\epsilon}_{\lambda'}(-\vec{q}) \\ &\Psi_3(\vec{0}))[Tr(t^\alpha t^\gamma t^\beta t^\gamma) - Tr(t^\alpha t^\gamma)Tr(t^\gamma t^\beta)] = \frac{5}{12} \frac{g^4 \Xi_{\lambda\lambda'}}{(2m_Q)^4} \tilde{B}_{s_2}(0)\tilde{A}_{s_1}(0)\tilde{B}_{s_4}(0)\tilde{A}_{s_3}(0) \\ &[2(\sigma_2\vec{\sigma} \cdot \vec{\epsilon})_{s_2s_1}(\sigma_2\vec{\sigma} \cdot \vec{\epsilon}')_{s_4s_3} + (\vec{\epsilon} \cdot \vec{\epsilon}')[(\sigma_2\vec{\sigma} \cdot \vec{v})_{s_2s_1}(\sigma_2\vec{\sigma} \cdot \vec{v})_{s_4s_3} - (\sigma_2)_{s_2s_1}(\sigma_2)_{s_4s_3}]] \ . \end{aligned}$$

For the **diagram e** we find

$$H_e \sim H_d \ .$$

Considering the **diagram f** we have

$$\begin{aligned} H_f &\sim -\frac{g^4}{2(2m_Q)^6} \Xi_{\alpha\beta\lambda\lambda'} (\bar{\Psi}_2(\vec{0})\gamma_\tau(-3\not{p} + m_Q)\not{\epsilon}_{\lambda'}(-\vec{q})(\not{p} - \not{q} + m_Q)\not{\epsilon}_\lambda(\vec{q})\Psi_1(\vec{0})) \\ &(\bar{\Psi}_4(\vec{0})\gamma^\tau\Psi_3(\vec{0}))Tr(t^\beta t^\alpha t^\gamma t^\gamma) = -\frac{1}{3} \frac{g^4 \Xi_{\lambda\lambda'}}{(2m_Q)^4} \tilde{B}_{s_2}(0)\tilde{A}_{s_1}(0)\tilde{B}_{s_4}(0)\tilde{A}_{s_3}(0) \\ &[\vec{\epsilon} \cdot \vec{\epsilon}'(\sigma_2\sigma_i)_{s_2s_1}(\sigma_2\sigma_i)_{s_4s_3}] \ , \end{aligned}$$

while considering the **diagram g** we have

$$\begin{aligned} H_g &\sim -\frac{g^4}{2(2m_Q)^6} \Xi_{\alpha\beta\lambda\lambda'} (\bar{\Psi}_2(\vec{0})\not{\epsilon}_{\lambda'}(-\vec{q})(\not{q}' - \not{p} + m_Q)\not{\epsilon}'_\lambda(-\vec{q})(3\not{p} + m_Q)\gamma_\tau\Psi_1(\vec{0})) \\ &(\bar{\Psi}_4(\vec{0})\gamma^\tau\Psi_3(\vec{0}))Tr(t^\beta t^\alpha t^\gamma t^\gamma) \sim H_f \ . \end{aligned}$$

For the **diagram h** we have

$$\begin{aligned} H_h &\sim \frac{g^4}{(2m_Q)^6} \Xi_{\alpha\beta\lambda\lambda'} (\bar{\Psi}_2(\vec{0})\not{\epsilon}_{\lambda'}(-\vec{q})(\not{q}' - \not{p} + m_Q)\gamma^\tau(\not{p} - \not{q} + m_Q)\not{\epsilon}_\lambda(\vec{q})\Psi_1(\vec{0})) \\ &(\bar{\Psi}_4(\vec{0})\gamma_\tau\Psi_3(\vec{0}))Tr(t^\alpha t^\gamma t^\beta t^\gamma) = -\frac{4}{3} \frac{g^4 \Xi_{\lambda\lambda'}}{(2m_Q)^4} \tilde{B}_{s_2}(0)\tilde{A}_{s_1}(0)\tilde{B}_{s_4}(0)\tilde{A}_{s_3}(0) \\ &[2(\sigma_2\vec{\sigma} \cdot \vec{\epsilon})_{s_2s_1}(\sigma_2\vec{\sigma} \cdot \vec{\epsilon}')_{s_4s_3} - (\vec{\epsilon} \cdot \vec{\epsilon}')[(\sigma_2\vec{\sigma} \cdot \vec{v})_{s_2s_1}(\sigma_2\vec{\sigma} \cdot \vec{v})_{s_4s_3} + (\sigma_2)_{s_2s_1}(\sigma_2)_{s_4s_3}]] \ . \end{aligned}$$

Coming to the **diagram i** we have

$$H_i \sim i \frac{g^4}{(2m_Q)^6} \Xi_{\alpha\beta\lambda\lambda'} Tr(t^\alpha t^\gamma t^\delta) f^{\beta\gamma\delta} (g^{\mu\rho}(q - 2p - q')^\nu + g^{\mu\nu}(2p + q')^\rho)$$

$$\begin{aligned}
& (\bar{\Psi}_2(\vec{0})\gamma_\rho(\not{p}' - \not{q} + m_Q)\not{\epsilon}_\lambda(\vec{q})\Psi_1(\vec{0})) (\bar{\Psi}_4(\vec{0})\gamma_\nu\Psi_3(\vec{0}))\epsilon_{\lambda'\mu}(-\vec{q}) \\
&= -\frac{3}{4}\frac{g^4\Xi_{\lambda\lambda'}}{(2m_Q)^4}[3(\sigma_2\vec{\sigma}\cdot\vec{\epsilon})_{s_2s_1})(\sigma_2\vec{\sigma}\cdot\vec{\epsilon}')_{s_4s_3}) + 2(\vec{\epsilon}\cdot\vec{\epsilon}')(\sigma_2\vec{\sigma}\cdot\vec{v})_{s_2s_1})(\sigma_2\vec{\sigma}\cdot\vec{v})_{s_4s_3})] \\
&\tilde{B}_{s_2}(0)\tilde{A}_{s_1}(0)\tilde{B}_{s_4}(0)\tilde{A}_{s_3}(0) ,
\end{aligned}$$

while for the **diagram j** we have

$$\begin{aligned}
H_j &\sim i\frac{g^4}{(2m_Q)^6}\Xi_{\alpha\beta\lambda\lambda'}Tr(t^\alpha t^\delta t^\gamma)f^{\beta\gamma\delta}(g^{\mu\rho}(q-2p-q')^\nu + g^{\mu\nu}(2p+q')^\rho) \\
&(\bar{\Psi}_2(\vec{0})\not{\epsilon}_\lambda(\vec{q})(\not{q}-\not{p}+m_Q)\gamma_\rho\Psi_1(\vec{0})) (\bar{\Psi}_4(\vec{0})\gamma_\nu\Psi_3(\vec{0}))\epsilon_{\lambda'\mu}(-\vec{q}) \\
&= -\frac{3}{4}\frac{g^4\Xi_{\lambda\lambda'}}{(2m_Q)^4}[3(\sigma_2\vec{\sigma}\cdot\vec{\epsilon})_{s_2s_1})(\sigma_2\vec{\sigma}\cdot\vec{\epsilon}')_{s_4s_3}) + 2(\vec{\epsilon}\cdot\vec{\epsilon}')(\sigma_2\vec{\sigma}\cdot\vec{v})_{s_2s_1})(\sigma_2\vec{\sigma}\cdot\vec{v})_{s_4s_3})] \\
&\tilde{B}_{s_2}(0)\tilde{A}_{s_1}(0)\tilde{B}_{s_4}(0)\tilde{A}_{s_3}(0) \sim H_i .
\end{aligned}$$

Now we can collect the ten operators into a single effective transition Hamiltonian

$H_{eff}|_{dist} \equiv \sum_x H_x$ getting

$$\begin{aligned}
H_{eff}|_{dist} &\sim -\frac{g^4\Xi_{\lambda\lambda'}}{(2m_Q)^4}\tilde{B}_{s_2}(0)\tilde{A}_{s_1}(0)\tilde{B}_{s_4}(0)\tilde{A}_{s_3}(0)\left[\frac{101}{6}(\sigma_2\vec{\sigma}\cdot\epsilon)_{s_2s_1})(\sigma_2\vec{\sigma}\cdot\epsilon')_{s_4s_3})\right. \\
&+\frac{29}{4}(\epsilon\cdot\epsilon')(\sigma_2\vec{\sigma}\cdot\vec{v})_{s_2s_1})(\sigma_2\vec{\sigma}\cdot\vec{v})_{s_4s_3}) - \frac{7}{3}\epsilon\cdot\epsilon'(\sigma_2\sigma_i)_{s_2s_1})(\sigma_2\sigma_i)_{s_4s_3}) \\
&\left.-\frac{1}{12}(\epsilon\cdot\epsilon')(\sigma_2)_{s_2s_1})(\sigma_2)_{s_4s_3})\right] .
\end{aligned}$$

Now we can compute the transition amplitudes in the \mathcal{T} rest frame which are given by

$$\delta(\vec{k} + \vec{k}')T_{\lambda,\alpha,\vec{k},\lambda',\beta,-\vec{k},\tau_{J,J_z},\vec{0}} \equiv \langle 0|a_{\lambda\alpha}(\vec{k})a_{\lambda'\beta}(\vec{k}')H_{eff}|\mathcal{T}_{J,J_z},\vec{0}\rangle . \quad (70)$$

Following the above introduced procedure and setting $\vec{k} = 2m_Q\vec{v}$, we have the creation operators in the gluon Fock space

$$\begin{aligned}
\langle 0|H_{eff}|\mathcal{T}_0,\vec{0}\rangle_{NR} &\simeq \frac{101}{18}\frac{g^4\Xi_{\lambda\lambda'}}{(2m_Q)^4}\Psi_{\mathcal{T}}(\vec{r}_i=0,\vec{P}=0)(\epsilon\cdot\epsilon') \\
&= \frac{101}{2^{\frac{5}{2}}3^2\pi^{\frac{7}{4}}m_Q^4d^3\delta^{\frac{3}{2}}}\alpha_S^2\Xi_{\lambda\lambda'}\delta_{\lambda\lambda'} \\
\langle 0|H_{eff}|\mathcal{T}_{1,1},\vec{0}\rangle_{NR} &\simeq 0 \\
\langle 0|H_{eff}|\mathcal{T}_{2,2},\vec{0}\rangle_{NR} &\simeq \frac{g^4\Xi_{\lambda\lambda'}}{\sqrt{3}(2m_Q)^4}\Psi_{\mathcal{T}}(\vec{r}_i=0,\vec{P}=0)\left[\frac{101}{6}\epsilon_+\epsilon'_+ + \frac{29}{4}v_+^2(\epsilon\cdot\epsilon')\right] \\
&= \frac{\alpha_S^2\Xi_{\lambda\lambda'}}{2^{\frac{7}{2}}3^{\frac{3}{2}}\pi^{\frac{7}{4}}m_Q^4d^3\delta^{\frac{3}{2}}}[202\epsilon_+\epsilon'_+ + 87v_+^2(\epsilon\cdot\epsilon')] . \quad (71)
\end{aligned}$$

Notice that the transition matrix element $\mathcal{T}_{1,1} \leftrightarrow 2g$ vanishes due to the charge conjugation invariance.

Since we have the relation

$$< 0 | a_{\zeta\alpha}(\vec{k}) a_{\zeta'\beta}(\vec{k}') \Xi_{\lambda\lambda'} | 0 > = \frac{\delta(\vec{k} + \vec{k}')}{4 m_Q} \delta^{\alpha\beta} (\delta_{\lambda\zeta} \delta_{\lambda'\zeta'} + \delta_{\lambda\zeta'} \delta_{\lambda'\zeta}) ,$$

where we have taken into account that, owing to the energy conservation, $k \simeq 2 m_Q$, we have

$$T_{\zeta,\alpha,\vec{k}, \zeta',\beta,-\vec{k}, \tau_{0,\vec{0}}} \simeq \frac{101}{2^{\frac{7}{2}} 3^2 \pi^{\frac{7}{4}} m_Q^5 d^3 \delta^{\frac{3}{2}}} \alpha_S^2 \delta^{\alpha\beta} \delta_{\zeta\zeta'} ,$$

and

$$T_{\zeta,\alpha,\vec{k}, \zeta',\beta,-\vec{k}, \tau_{2,2,\vec{0}}} \simeq \frac{\alpha_S^2}{2^{\frac{9}{2}} 3^{\frac{3}{2}} \pi^{\frac{7}{4}} m_Q^5 d^3 \delta^{\frac{3}{2}}} \delta^{\alpha\beta} [202 \epsilon_{\zeta+}(\vec{k}) \epsilon_{\zeta'+}(-\vec{k}) + 87 v_+^2 (\vec{\epsilon}_\zeta(\vec{k}) \cdot \vec{\epsilon}_{\zeta'}(-\vec{k}) \epsilon')] .$$

Computing the Drell-Yan production cross section we need the average of the values of $|T|^2$ over the helicity and color states of the gluons and, for \mathcal{T}_2 , over the momentum directions. Thus, we have

$$\overline{|T_{h,\alpha,\vec{v}, h',\beta,-\vec{v}, \tau_{0,\vec{0}}}|^2} \simeq 10^{-3} \frac{\alpha_S^4}{m_Q^{10} d^6 \delta^3} , \quad (72)$$

while for \mathcal{T}_2 we must consider the dependence of the gluon polarization vectors in the laboratory frame on the Euler angles describing the orientation of the frame whose axes are the vectors \vec{v} and $(\vec{\epsilon}_+ + \vec{\epsilon}_-)/\sqrt{2}$, the vectors $\vec{\epsilon}_\pm$ being defined in Eq. (58). In the laboratory frame the vector \vec{v} has components $\sin \beta \cos \alpha$, $\sin \beta \sin \alpha$, $\cos \beta$ while the $+$ components of the polarization vectors with helicity ζ are

$$\epsilon_{+,\zeta}(\pm \vec{k}) \equiv \frac{\epsilon_{x,\zeta}(\pm \vec{k}) + i \epsilon_{y,\zeta}(\pm \vec{k})}{\sqrt{2}} = e^{\pm i(\alpha + \zeta \gamma)} \frac{\cos \beta + \zeta}{\sqrt{2}} .$$

Therefore

$$\frac{1}{8\pi^2} \int_0^{2\pi} d\alpha d\gamma \int_{-1}^1 d\cos \beta |202 \epsilon_{\zeta+}(\vec{k}) \epsilon_{\zeta'+}(-\vec{k}) + 87 \delta_{\zeta\zeta'} v_+^2|^2 \simeq 5.4 \cdot 10^3 + 3.1 \cdot 10^4 \delta_{\zeta\zeta'} ,$$

and hence

$$\overline{|T_{h,\alpha,\vec{v}, h',\beta,-\vec{v}, \tau_{2,2,\vec{0}}}|^2} \simeq 3.4 \cdot 10^{-3} \frac{\alpha_S^4}{m_Q^{10} d^6 \delta^3} . \quad (73)$$

Inserting into Eq. (15) the results given in Eq.'s (72) and (73) and taking into account the spin degeneracy of \mathcal{T}_2 one gets a production cross section which is roughly a factor 17 greater than that of \mathcal{T}_0 .

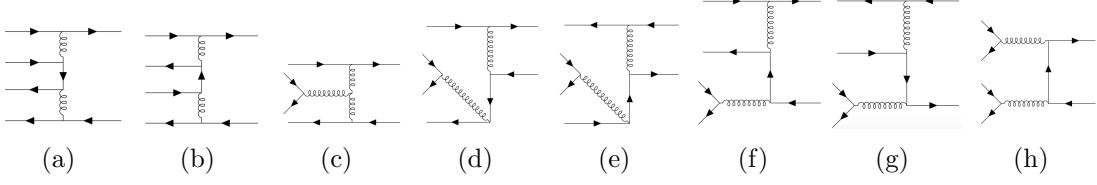


Figure 3: The transition $\mathcal{T} \leftrightarrow q\bar{q}$.

D.2 The transition $\mathcal{T} \leftrightarrow q\bar{q}$.

Now we come to the light parton quarks noting that at the same order one might consider the exclusive decay of the tetra-Quark into a $Q\bar{Q}$ pair. The rate of this decay which is of the fourth order in α_S is determined by all the diagrams in Figure 3. It is not difficult to verify that the decay rate is of the order of $\alpha_S^4/(m_Q^8 \delta^3 d^6)$, that is of few electron-Volt and hence negligible.

In fact we are interested in the transition amplitude $\mathcal{T} \rightarrow q\bar{q}$ for light quarks which determines the parton quark contribution to the production cross section of the \mathcal{T} . This is interesting even if we know that the corresponding luminosity is by almost two orders of magnitude smaller than that of two gluons.

It is apparent that the effective Hamiltonian only corresponds to diagram (h). We shall systematically follow the simplifications and notations used in the previous Section replacing the gluons by the light quarks whose mass we disregard. We denote by a and b the destruction operators of the light quarks and anti-quarks and neglect their masses. Then we have the effective Hamiltonian

$$\begin{aligned}
H_{esc} &\simeq -\frac{g^4}{(2m_Q)^5} \tilde{B}_{s_4,c}(\vec{0}) \tilde{A}_{s_3,d}(\vec{0}) \tilde{B}_{s_2,f}(\vec{0}) \tilde{A}_{s_1,g}(\vec{0}) (\bar{U}_{s_4} \gamma_2 \gamma^\nu U_{s_3}) (\bar{U}_{s_2} \gamma_2 \gamma^\mu U_{s_1}) \\
&t_{cd}^\alpha t_{fg}^\beta (t^\alpha t^\beta)_{lm} \int \frac{d\vec{q}}{2q} a_{h,m}^\dagger(\vec{q}) b_{h',l}^\dagger(-\vec{q}) (\bar{u}_h(\vec{q}) \gamma_\mu \psi \gamma_\nu v_{h'}(-\vec{q})) \\
&= \frac{\pi^2 \alpha_S^2}{3 m_Q^5} \tilde{B}_{s_4,c}(\vec{0}) \tilde{A}_{s_3,d}(\vec{0}) \tilde{B}_{s_2,f}(\vec{0}) \tilde{A}_{s_1,g}(\vec{0}) (\sigma_2 \sigma_i)_{s_2 s_1} (\sigma_2 \sigma_j)_{s_4 s_3} \\
&\int \frac{d\vec{q}}{2q} a_{h,m}^\dagger(\vec{q}) b_{h',m}^\dagger(-\vec{q}) (\bar{u}_h(\vec{q}) \gamma_i \psi \gamma_j v_{h'}(-\vec{q})) .
\end{aligned} \tag{74}$$

Following the same line as that in Appendix D.1 we compute the light quark creation operators

$$\begin{aligned}
\langle 0 | H_{esc} | \mathcal{T}_0, \vec{0} \rangle_{NR} &\simeq -\frac{\pi^2 \alpha_S^2}{9 m_Q^5} \Psi_{\mathcal{T}}(\vec{r}_i = 0, \vec{P} = 0) \int \frac{d\vec{q}}{2q} a_{h,m}^\dagger(\vec{q}) b_{h',m}^\dagger(-\vec{q}) \\
&(\bar{u}_h(\vec{q}) \gamma_i \psi \gamma_i v_{h'}(-\vec{q})) = -\frac{\alpha_S^2}{9 \cdot 2^{\frac{3}{2}} \pi^{\frac{7}{4}} d^3 \delta^{\frac{3}{2}} m_Q^5} \int \frac{d\vec{q}}{2q} a_{h,m}^\dagger(\vec{q}) b_{h',m}^\dagger(-\vec{q}) (\bar{u}_h(\vec{q}) \gamma_i \psi \gamma_i v_{h'}(-\vec{q})) \\
&= \frac{\alpha_S^2}{9 \cdot 2^{\frac{3}{2}} \pi^{\frac{7}{4}} d^3 \delta^{\frac{3}{2}} m_Q^5} \int \frac{d\vec{q}}{2q} a_{h,m}^\dagger(\vec{q}) b_{h',m}^\dagger(-\vec{q}) (\bar{u}_h(\vec{q}) \psi v_{h'}(-\vec{q})) \\
\langle 0 | H_{esc} | \mathcal{T}_{1,1}, \vec{0} \rangle_{NR} &\simeq 0 \\
\langle 0 | H_{esc} | \mathcal{T}_{2,2}, \vec{0} \rangle_{NR} &\simeq -\frac{\alpha_S^2}{3^{\frac{3}{2}} \sqrt{2} \pi^{\frac{7}{4}} d^3 \delta^{\frac{3}{2}} m_Q^5} \int \frac{d\vec{q}}{2q} a_{h,m}^\dagger(\vec{q}) b_{h',m}^\dagger(-\vec{q})
\end{aligned}$$

$$(\bar{u}_h(\vec{q})(\psi + i(v_x\gamma_y + v_y\gamma_x)) v_{h'}(-\vec{q})) . \quad (75)$$

Notice that the transition matrix element $\mathcal{T}_{1,1} \leftrightarrow p\bar{p}$ vanishes for any parton choice. This means that \mathcal{T}_1 is practically not produced at the LHC.

Then we have

$$\begin{aligned} T_{h,a,\vec{k}, h',b,-\vec{k}, \tau_{0,\vec{0}}} &\simeq \frac{\alpha_S^2}{9 \cdot 2^{\frac{7}{2}} \pi^{\frac{7}{4}} d^3 \delta^{\frac{3}{2}} m_Q^6} \delta_{ab} (\bar{u}_h(\vec{k}) \psi v_{h'}(-\vec{k})), \\ T_{h,a,\vec{k}, h',b,-\vec{k}, \tau_{2,2,\vec{0}}} &\simeq \frac{\alpha_S^2}{3^{\frac{3}{2}} 2^{\frac{5}{2}} \pi^{\frac{7}{4}} d^3 \delta^{\frac{3}{2}} m_Q^6} \delta_{ab} (\bar{u}_h(\vec{k}) (\psi + i(v_x\gamma_y + v_y\gamma_x)) v_{h'}(-\vec{k})), \end{aligned}$$

where $\vec{k} = 2 m_Q \vec{v}$.

Now we can compute the mean square transition amplitudes

$$\begin{aligned} \overline{|T_{h,m,\vec{v}, h',l,-\vec{v}, \tau_{0,\vec{0}}}|^2} &\simeq \frac{\alpha_S^4}{3^5 2^7 \pi^{\frac{7}{2}} d^6 \delta^3 m_Q^{12}} \int \frac{d\vec{v}}{4\pi} m_Q^2 \text{Tr}[(\gamma_0 + \psi) \psi (\gamma_0 - \psi) \psi] = 0 \\ \overline{|T_{h,m,\vec{v}, h',l,-\vec{v}, \tau_{2,2,\vec{0}}}|^2} &\simeq \frac{\alpha_S^4}{3^4 2^5 \pi^{\frac{7}{2}} d^6 \delta^3 m_Q^{12}} \int \frac{d\vec{v}}{4\pi} m_Q^2 \text{Tr}[(\gamma_0 + \psi) (\psi + i(v_x\gamma_y + v_y\gamma_x)) \\ &(\gamma_0 - \psi) (\psi - i(v_x\gamma_y + v_y\gamma_x))] = \frac{\alpha_S^4}{3^4 10 \pi^{\frac{7}{2}} d^6 \delta^3 m_Q^{10}} \simeq 1.2 \cdot 10^{-3} \frac{\alpha_S^4}{m_Q^{10} d^6 \delta^3} . \end{aligned} \quad (76)$$

Thus, the mean squared transition amplitude between \mathcal{T}_2 and a $q\bar{q}$ pair is about half of that in two gluons. Therefore, since the gluon-gluon luminosity is about two orders of magnitude greater than the quark-anti-quark one, this last contribution can be disregarded.

Acknowledgements

The Author is in debt of gratitude to E. Santopinto for constant help and encouragement, to S. Frixione, S. Marzani and G. Ridolfi for their crucial help on the parton-parton luminosity calculations. He is also in debt to F. Parodi for information on detection efficiencies at the LHC.

References

- [1] F. Okiharu, T. Doi, H. Ichie, H. Iida, N. Ishii, M. Oka, H. Suganuma and T. Takahashi, *Tetraquark and Pentaquark Systems in Lattice QCD*, J. Mod. Phys. **7** (2016) 774, [hep-ph/0507187v1].
- [2] M.N. Anwar, J. Ferretti, F.K. Guo, E. Santopinto and B.S. Zuo, *Spectroscopy and decays of the fully-heavy tetraquarks*, Eur. Phys. J. C **78** (2018) 647, [hep-ph/1710.02540v4].

- [3] D. Molina, M. De Sanctis, C. Fernández-Ramírez and E. Santopinto, *Bottomonium spectrum with a Dirac potential model in the momentum space*, Eur. Phys. J. C. **80** (2020) 6.
M. A. Bedolla, J. Ferretti, C. D. Roberts and E. Santopinto, *Spectrum of fully-heavy tetraquarks from a diquark+antidiquark perspective*, Eur. Phys. J. C **80** (2020) 1004, [hep-ph/1911.00960].
P. Lundhammar and T. Ohlsson, *Nonrelativistic model of tetraquarks and predictions for their masses from fits to charmed and bottom meson data*, Phys. Rev. D **102** (2020) 054018, [hep-ph/2006.09393].
G. Yang, J. Ping, and J. Segovia, *Exotic resonances of fully-heavy tetraquarks in a lattice-QCD inspired quark model*, Phys. Rev. D **104** (2021) 1,014006, [hep-ph/2104.08814].
J.-M. Richard, *Fully-heavy tetraquarks and other heavy multiquarks*, [hep-ph/2105.02503].
- [4] LHCb Collaboration, *Observation of structure in the J/ψ -pair mass spectrum*, Science Bulletin **65** (2020) 1983 [hep-ex/006.16957v1].
- [5] C. Becchi, A. Giachino, L. Maiani and E. Santopinto, *Search for $b\bar{b}b\bar{b}$ tetraquark decays in 4 muons, B^+B^- , $B^0\bar{B}^0$ and $B_s^0\bar{B}_s^0$ channels at LHC* Phys. Lett. **B806** (2020) 135495, [hep-ph/2002.11077].
- [6] C. Becchi, J. Ferretti, A. Giachino, L. Maiani and E. Santopinto, *A study of $cc\bar{c}\bar{c}$ tetraquark decays in 4 muons and in $D^{(*)}\bar{D}^{(*)}$ at LHC*, Phys. Lett. **B811** (2020) 135952, [hep-ph/2006.14388].
- [7] C. Becchi, G. Ridolfi, *An Introduction to Relativistic Processes and the Standard Model of Electroweak Interaction [Second Edition]*, Springer-Verlag Italia (2014).
- [8] LHCb Collaboration, *Measurement of forward J/ψ production cross-sections in pp collisions at $\sqrt{s} = 13$ TeV*, JHEP **10** (2016) 172, [hep-ex/1509.00771v5].
LHCb Collaboration, *Measurement of the $\eta_c(1S)$ production cross-section in pp collisions at $\sqrt{s} = 13$ TeV*, Eur. Phys. J. C **80** (2020) 191.
- [9] LHCb Collaboration, *Measurement of Υ production cross-sections in pp collisions at $\sqrt{s} = 13$ TeV*, JHEP **07** (2018) 134, [hep-ex/1804.09214v2].
- [10] ATLAS Collaboration, *Measurement of the transverse momentum distribution of Drell-Yan lepton pairs in proton-proton collisions at $\sqrt{s} = 13$ TeV with the ATLAS detector*, Eur. Phys. J. C **80** (2020) 616, [hep-ex/1912.02844v2].
- [11] J.M. Campbell, J.W. Huston and W.J. Stirling, *Hard Interactions of Quarks and Gluons: a Primer for LHC Physics*, Rept. Prog. Phys. **70** (2007) 89, [hep-ph/0611148v1].
A.D. Martin, W.J. Stirling, R.S. Thorne and G. Watt, *Parton distributions for the LHC*, Eur. Phys. J. C **63** (2009), 189 [hep-ph/arXiv:0901.0002v3].

- [12] H. L. Lai, M. Guzzi, J. Huston, Z. Li, P. M. Nadolsky, J. Pumplin and C. P. Yuan, *New parton distributions for collider physics*, Phys. Rev. D **82** (2010) 074024, [hep-ph/1007.2241v3].
M. Guzzi *et al.*, *CTEQ-TEA parton distribution functions with intrinsic charm*, [hep-ph/1810.00264v1].
- [13] R.D. Ball, *Resummation of hadroproduction cross-sections at high energy* Nuclear Phys. **B796** (2008) 137.
R. D. Ball *et al.* [NNPDF Collaboration], *Parton distributions for the LHC run II*, JHEP **04** (2015) 040, [hep-ph/1410.8849].
R. D. Ball *et al.* [NNPDF Collaboration], *Parton distributions from high-precision collider data* [hep-ph/1706.00428v2].
- [14] D. B. Clark, E. Godat and E.L. Olness, *A Mathematica reader for Parton Distribution Functions*, Computer Physics Communications 216 (2017) 126.
- [15] LHCb Collaboration, *Measurement of the b -quark production cross-section in 7 and 13 TeV pp collisions*, Phys. Rev. Lett. **118** (2017) 5, [hep-ex/1612.05140v9].
- [16] LHCb Collaboration, *Measurement of the J/ψ pair production cross-section in pp collisions at $\sqrt{s} = 13$ TeV*, JHEP **06** (2017) 047, [hep-ex/1612.07451v3].
- [17] CMS Collaboration, *Measurement of the $Y(1S)$ pair production cross section and search for resonances decaying to $Y(1S)\mu^+\mu^-$ in proton-proton collisions at $\sqrt{s} = 13$ TeV*, Phys. Lett. **B808** (2020) 135578, [hep-ex/2002.06393].
- [18] A. Deur, S. J. Brodsky and G. F. de Teramond, *The QCD Running Coupling*, Prog. Part. Nucl. Phys. **90** (2016) 1-74, [hep-ph/1604.08082].